Social exploitation of extensive, ephemeral, environmentally controlled prey patches by super-groups of rorqual whales

David E. Cade[a,b,*], James A. Fahlbusch[a,c], William K. Oestreich[a], John Ryan[d], John Calambokidis[c] , Ken P. Findlay[e,f], Ari S. Friedlaender[b], Elliott L. Hazen[g], S. Mduduzi Seakamela[h], Jeremy A. Goldbogen[a]

[a]Hopkins Marine Station, Stanford University, CA, U.S.A.
[b]Institute of Marine Science, University of California, Santa Cruz, U.S.A.
[c]Cascadia Research Collective, Olympia, WA, U.S.A.
[d]Monterey Bay Aquarium Research Institute, CA, U.S.A.
[e]Oceans Economy, Cape Peninsula University of Technology, Cape Town, South Africa
[f]MRI Whale Unit, Department of Zoology and Entomology, University of Pretoria, South Africa
[g]Environmental Research Division/Southwest Fisheries Science Center/National Marine Fisheries Service/National Oceanic and Atmospheric Administration, Monterey, CA, U.S.A.
[h]Department of Environment, Forestry and Fisheries, Branch: Oceans and Coasts, Victoria & Alfred Waterfront, Cape Town, South Africa

*Corresponding author. davecade@stanford.edu

Highlights

•Large, dense prey patches were found near supergroups of rorqual whales.
•Ephemeral patches formed when surface features intersected with bathymetry.
•Blue whales increased social call production during observed aggregation events.
•Rorqual whale foraging appears to be enhanced when social information is utilized.

ABSTRACT

Large groups of animals aggregate around resource hotspots, with group size often influenced by the heterogeneity of the environment. In most cases, the foraging success of individuals within groups is interdependent, scaling either constructively or destructively with group size. Here we used bio-logging tags, acoustic prey-mapping, passive acoustic recording of social cues and remote sensing of surface currents to investigate an alternative scenario in which large, dense aggregations of SE Atlantic humpback whales and NE Pacific blue whales were each associated with ephemeral krill aggregations large enough such that their availability to predators appeared to be influenced more by environmental features than by consumption, implying independence of group size and consumption rates. We found that the temporal scale and spatial extent of oceanographic drivers were consistent with the temporal scale and locations of predator aggregations, and additionally found that groups formed above bathymetric features known to

promote zooplankton concentration. Additionally, we found calling behavior counter-indicative of competition: blue whale foraging calls were anomalously high during observed aggregation time periods, suggesting signaling behavior that could alert conspecifics to the location of high-quality resources. Modeled results suggest that the use of social information reduces the time required for individuals to discover and exploit high-quality resources, allowing for more efficient foraging without apparent costs to the caller. Thus, rorqual whales foraging in these environments appear to exhibit a social foraging strategy whereby a behavior with negligible individual costs (signaling) provides information that enhances group foraging efficiency. The population-density dependence of this social foraging strategy may help explain why some rorqual species were at first slow to recover from human exploitation, but have since increased more rapidly.

KEY WORDS

blue whales, environmentally controlled depletion, FTLE, marine hot spots, humpback whales, information sharing, patchiness, social foraging

INTRODUCTION

Animals are distributed relative to the resources they rely upon, often scaling in number with resource availability (Bernstein, Kacelnik, & Krebs, 1991; Johnson et al., 2002; McNamara & Houston, 1990) and with the spatial and temporal heterogeneity of resource distribution (Johnson et al., 2002). Large aggregations of animals form for a wide variety of reasons including mating (Johannes et al., 1999; Swartz & Jones, 1981), proximity to a limiting resource (Valeix, Chamaillé-Jammes, & Fritz, 2007), physical forcing (Hofmann & Murphy, 2004), increased foraging opportunities (Brown, 1988; Giraldeau & Caraco, 2000) and either active predator defense (Clark & Robertson, 1979; Magurran, 1990) or passive predator avoidance (Laundré, 2010); generally these benefits result in an increased evolutionary fitness that

outweighs the costs associated with dividing available resources among the group (Lang & Farine, 2017; Parrish & Edelstein-Keshet, 1999).

Social foraging frameworks typically model depletable (i.e. consumable) patches of various sizes, and have been shown to apply in systems as diverse as bats (Egert-Berg et al., 2018), ants (Flanagan et al., 2011; Gordon, Rosengren, & Sundström, 1992), finches (Livoreil & Giraldeau, 1997) and sea-birds (Buckley, 1997; Pöysä, 1992). An underlying assumption of these frameworks is that an individual's resource intake is reduced by the presences of interacting conspecifics that compete for a resource pool that is depleted more rapidly as group size increases.

Baleen whales (parvorder: Mysticeti) are the world's largest predators, exhibit both individual and group foraging behavior, have large vocal repertoires (Dunlop, Cato, & Noad, 2008; Fournet, Szabo, & Mellinger, 2015) that can be detected over large ranges (Miller et al., 2019; Stafford, Fox, & Clark, 1998), and, as capital-breeding bulk filter feeders, require dense concentrations of seasonally available prey that exhibit both spatial (Friedlaender et al., 2020; Hazen et al., 2009; Irvine et al., 2019; Kirchner et al., 2018; Piatt & Methven, 1992; van der Hoop et al., 2019) and temporal patchiness (Abrahms et al., 2019; Becker et al., 2014; Dodson et al., 2020; Fossette et al., 2017). Social foraging frameworks would thus be expected to apply to baleen whale predator/prey systems, and the development of bio-logging devices and hydroacoustic prey mapping have recently made it possible to study both the behavior of these enigmatic predators and the distribution of their prey quantitatively and simultaneously *in situ* (e.g. Goldbogen et al., 2019; Owen et al., 2017).

Variously-sized aggregations of baleen whales around patchy resources are commonly reported at a wide variety of spatial scales and with varying degrees of temporal cohesion (e.g. Baines, Reichelt, & Griffin, 2017; Fiedler et al., 1998; Findlay et al., 2017; Hucke-Gaete et al., 2004; Jurasz & Jurasz, 1979; Littaye et al., 2004; Lomac-MacNair & Smultea, 2016; Mastick, 2016; Newton & DeVogelaere, 2013; Nowacek et al., 2011; Piatt & Methven, 1992; Schoenherr, 1991; Visser et al., 2011; Whitehead, 1983). Humpback whales (*Megaptera novaeangliae*), for example, are flexible foragers that commonly prey on both relatively static patches of krill (Euphausiids) as well as mobile schooling fish. Humpback whales

have been observed feeding both alone and in large groups with synchronized and apparently coordinated behaviors that serve to concentrate schools of fish before individuals lunge into the school to capture as many as possible in a single mouthful. The size of fish schools can influence the size of the groups (Fig 1) – individuals foraging in the same region can pursue one small school, engulf it and move on to the next (e.g. Cade et al., 2020; Weinrich, Schilling, & Belt, 1992), or a group of individuals can lunge several times on the same large school of fish (e.g. Cade et al., 2020; Jurasz & Jurasz, 1979; Kirchner et al., 2018; Wiley et al., 2011). Though rigorous tests of social foraging theories in these systems have yet to be completed, both of these strategies appear to fit model assumptions (e.g. Giraldeau & Caraco, 2000), with patches that are depleted over time and individual decisions driven by the tradeoffs involved in resource sharing.

In marine environments, however, the heterogeneity of the ecosystem and its resource availability can be controlled by rapid turnover of nutrients and cyclical physical processes (Haury, McGowan, & Wiebe, 1978). This leads to spatially and temporally restricted blooms in resource availability and encourages aggregations of mid-trophic level animals to form and disperse under the influence of cyclical environmental processes such as upwelling (Benoit-Bird, Waluk, & Ryan, 2019), currents (Lévy, Franks, & Smith, 2018), surface winds (Blukacz, Shuter, & Sprulesc, 2009) and tides (Cotté & Simard, 2005; Dustan & Pinckney Jr, 1989; Johnston, Thorne, & Read, 2005). The ocean, then, is a likely environment in which to find ephemeral patches of prey whose foraging quality is driven more strongly by the environment than by predation (Benoit-Bird & McManus, 2012). These conditions suggest an additional social foraging scenario in which patch quality and resource availability are not affected by group size, encouraging alternate social foraging strategies wherein it is advantageous for individuals to cooperate by communicating the location of ephemeral resources when they are available (Torney, Berdahl, & Couzin, 2011; Wilson et al., 2018). In this scenario, alerting conspecifics to the location of extensive, ephemeral resources would have low individual costs but high collective advantages. We refer to this scenario as "environmentally controlled," and examine evidence that large aggregations of two species of rorqual whales foraging within extensive but ephemeral krill patches could be an exemplar of this ephemeral prey patch model.

Beginning in 2011, spatially constricted, numerically dense concentrations of humpback whales have been reported seasonally in the Benguela Current region off South Africa's west coast (Findlay et al., 2017). Known as "super-groups", these aggregations consist of 20 to >200 whales, each of which is within five body lengths of a conspecific. These aggregations were shown to be associated with extraordinarily dense, abundant and thick aggregations of prey that were more uniform in distribution than nearby prey patches, leading to a doubling of intake rates for animals foraging in those patches (Cade et al., 2021). Here we investigate the bathymetry and surface currents surrounding these groups, hypothesizing that surface currents interact with bathymetric features in the region on spatial and temporal scales consistent with those of each observed group.

In contrast to humpback whales, blue whales (*Balaenoptera musculus*) are typically observed singly or in pairs, forage almost exclusively on krill (Kawamura, 1980) and are not known to engage in behaviors, such as prey-herding, that may be more effective in larger groups (Mastick, 2016). These world's largest predators are also rarely observed in close proximity: 21 out of 22 studies synthesized by Ramm (2018, see Table 2 within) observed mean blue whale group sizes of 1-2 individuals, and in 963 field surveys over 20 years by our field team, less than 6% encountered at least 25 blue whales over the course of the day most of which involved separate encounters separated by several miles. However, on 14 and 16 August 2017, dense aggregations of 15-40 blue whales, surfacing within a 1 km radius area, were observed in Monterey Bay, CA, associated with thick, dense, evenly distributed prey patches (Cade et al., 2021). As with the humpback whale groups in South Africa, we hypothesized that the observed blue whale aggregations were located near constrictive bathymetric features that would serve to aggregate prey on multi-hour temporal scales consistent with the observed time scales of group formation.

Blue whale (and other rorqual) prey intake rate (λ) is constrained biomechanically, physiologically and environmentally (Fig 2). While prey processing time is a biomechanical constraint that appears to depend on engulfment volume (regardless of prey density in the volume, Kahane-Rapport et al., 2020) and surface time is a physiological constraint that depends on the characteristics of an individual patch (Hazen, Friedlaender, & Goldbogen, 2015), the search time required to find appropriately dense prey is limited by

the animal's ability to find and detect food (Wilson et al., 2018) that can be dispersed across a home range that spans hundreds of kilometers (Abrahms et al., 2019; Mate, Lagerquist, & Calambokidis, 1999), making the time to find high-quality patches the dominant temporal factor influencing λ. While it is not known which sensory systems blue whales use to locate good forage areas, it has been shown that signaling behavior that recruits conspecifics to a food resource can be an evolutionarily stable strategy in spatially and temporally dynamic environments like those in marine krill ecosystems (Torney et al., 2011). We thus hypothesized that we would detect increased signaling behavior from blue whales during the observed aggregation events. To test this hypothesis, we used data from a continuously recording hydrophone in Monterey Bay, and we constructed models to examine how such signaling behavior would affect overall prey intake and influence the time scales of group formation.

METHODS

Super-group predator/prey dynamics

We investigated aggregations of rorqual whales in two eastern boundary-current upwelling ecosystems: 11 instances of humpback whale super-groups in the Benguela Current off South Africa's west coast in 2015 and 2016 and two instances of blue whale super-groups in Monterey Bay off the US west coast in 2017 (Fig 3). These aggregations are distinct from other contemporary descriptions of large groups in the extraordinary density of animals within a small region of open ocean such that animals must interact with each other as they are foraging (Video S3). Specifics of both types of aggregations are detailed in Cade et al. (2021).

Formation and dispersion of whale aggregations were observed opportunistically from research vessels in each ecosystem. To examine foraging behavior within and outside of super-groups we attached 17 integrated 3D accelerometer and video tags to individual blue whales for time periods of ~ 2 – 20 hrs, six of which were whales foraging within super-groups in 2017, and we tagged an additional 22 blue whales in the same region in 2018 (no super-groups were observed in 2018). Prey data were collected using a multi-

frequency, split-beam fisheries acoustic system (Simrad EK60s or EK80s) ensonifying the water column below a vessel within 500 m of foraging whales in both ecosystems, and data collected near super-groups were compared to data collected near feeding whales not aggregated into super-groups. Aggregations of krill, dominated by large patches > 10 m thick and 1 km across, were identified in acoustic echograms using the SHAPES school detection algorithm (Barange, 1994; Coetzee, 2000) and dB differencing techniques (Jarvis et al., 2010), and were analyzed at predator-specific spatial scales relevant to the unique foraging mechanisms of lunge-feeding rorqual whales (detailed description of the "whale-scale" method, including conversion from acoustic units to estimated biomass in Cade et al., 2021).

Bathymetry

Bathymetric data for inset Monterey Bay map in Figs 3A and 4A were gridded to 25 m resolution (from source data sets having variable resolutions) and provided by the Monterey Bay Aquarium Research Institute (MBARI). Remaining Monterey Bay data were derived from a one-third arcsecond digital elevation model from the NOAA National Geophysical Data Center, accessed at: https://www.ncei.noaa.gov/metadata/geoportal/rest/metadata/item/gov.noaa.ngdc.mgg.dem:3544/html. Data in Fig 3A were plotted in R with contours from 50 to 1600 meters depth at 50 m intervals, and data in Figs 2B as well as all 3D plots were based on contours generated by the contour function in Matlab v2014a at 3 m intervals to 120 m, 10 m intervals to 1000 m, then 50 m after that. Three-dimensional data were plotted in Echoview v10 from the Matlab generated contours using a 10x vertical exaggeration and the Echoview 1xx color scheme colored for gray scale display (min depth: -1000 m, max depth 7000 m).

Depth soundings in the South African study region at approximately 5 km resolution (ungridded) were provided by the South African Naval Hydrographic Office for exclusive use of this project. Data were gridded using the geoloc2grid function in Matlab at 22.5 arcsecond resolution, then contoured and plotted as above except with vertical exaggerations as noted in figure legends for clarity. The coastline depicted in Fig 3B is from Wessel and Smith (1996).

Social cue production

We utilized a continuous passive acoustic monitoring system from the Monterey Accelerated Research Station (MARS) cabled observatory hydrophone (Oestreich et al., 2020; Ryan et al., 2016) to examine the production of acoustic cues by blue whales temporally proximate to super-group observations. This omnidirectional hydrophone has a bandwidth of 10 Hz to 200 kHz and has been sampling nearly continuously at 256 kHz from late July 2015 to the present. The hydrophone is situated on Smooth Ridge (36°42.75'N, 122°11.21'W; depth 891 m), spatially located both in blue whale foraging habitat generally (Croll et al., 2005), as well as the field effort for this study specifically (Fig 3). Blue whale calls are low-frequency and have been recorded at distances of hundreds of km (Miller et al., 2019; Stafford et al., 1998) so any calls produced by the whales in our study (super-group distances were 16.8 and 14.0 km while the max distance from any feeding whale was 48.9 km) were likely to be recorded. Sound propagation loss modeling results for blue whale B-calls (Oestreich et al., 2020) and humpback song (Ryan et al., 2019) at the same instrument indicate that the locations of observed super-groups are well within the sampling radius of the MARS hydrophone. Blue whale calls have the bulk of their energy below 200 Hz (Oleson, Wiggins, & Hildebrand, 2007), so acoustic data were decimated by a factor of 128 to produce a 2 kHz product (via software available at: https://bitbucket.org/mbari/soundscape-decimate-notebook/src/master/).

D calls in blue whales, which are thought to be associated with feeding (Oleson, Calambokidis, et al., 2007), are characterized by a steep downsweep in frequency in the 20-120 Hz range over ~2-7 seconds (Oleson, Wiggins, et al., 2007), and high calling rates have been associated with aggregating blue whales (Miller et al., 2019). We manually audited spectrograms (FFT window size = 1024, Hann window, overlap = 95%) from data recorded August 1st through September 15th in both 2017 and 2018 to identify D calls, distinguishable from fin whale calls by the length of the signal (Huang et al., 2016) and from downsweeping humpback whale song segments by the context within the spectrograms (Fig 6A). We aggregated D call counts into one-hour bins to calculate a mean diel cycle during this time period (Fig 6B). We calculated D call rate anomalies (Fig 6C) by subtracting the mean 24-hour trend from the hourly-binned D call counts and then reduced noise by averaging these hourly anomalies into 4-hour bins.

Oceanographic features

We examined the oceanographic conditions temporally proximate to blue whale super-group observations in Monterey Bay in three ways: 1) using backwards-in-time Finite-Time Lyapunov Exponents (FTLE) to perform a Lagrangian analysis of predicted particle accumulation based on surface currents measured by the High-Frequency (HF) radar data along the California coast (Paduan & Rosenfeld, 1996), 2) examining hourly plots of surface current rotation rates (vorticity), also derived from HF radar, and 3) assessing *in situ* Acoustic Doppler Current Profiler (ADCP) data from a mooring at the mouth of Monterey Bay over Monterey Canyon (Fig 3A; 36.755°N, 122.03°W).

Surface current data for deriving FTLE and vorticity data were downloaded from the Southern California Coastal Ocean Observing System (SCCOOS, http://www.sccoos.org/data/hfrnet/) at hourly resolution (cells 6 km on a side) using a polygon bounded by parallels and meridians at 37.25˚N, 36.0˚N, 123.0˚W and 121.5˚W. This polygon encompasses all feeding areas utilized by tagged blue whales from 2017 and 2018 in MRY and is within the coverage range of HF radar platforms. HF radar, a terrestrial-based remote sensing platform, overcomes the spatial and temporal resolution constraints of traditional remote sensing platforms (e.g., satellites, buoys) by providing fine-scale measurements of surface current movements (hourly, 2-6 km resolution) in areas that overlap with typical blue whale habitat (up to 200 km offshore). It works by reflecting electromagnetic waves off the surface of the ocean to determine the two-dimensional speed and direction of water moving at the surface (Chapman et al., 1997), and has been used to look at the relationship between foraging behavior and surface convergent features (Abrahms et al., 2018; Oliver et al., 2019; Scales et al., 2014; Scales et al., 2017).

To facilitate a Lagrangian analysis in the calculation of FTLE, we restored data gaps in the HF radar surface current measurements using the algorithms described in Ameli and Shadden (2019), selecting a concave hull (alpha shape radius of 10 km) and excluding land. Using the restored surface current data, we calculated the backward-in-time FTLE using TRACE (http://transport.me.berkeley.edu/trace/), a Lagrangian analysis tool that follows the methodology described in Shadden et al. (2005; 2009). We used a tracer resolution of 10 times the spatial resolution of the HF radar data (sensu Shadden et al., 2009), and

applied a free-slip boundary condition to tracers near land. Tracer advection used a bilinear spatial interpolation and an adaptive 4th order Runge-Kutta-Fehlberg integration method. At every hourly time-step, the trajectories of the evenly spaced grid of tracers were integrated for the preceding 6-, 12-, 24- or 96-hour period, and FTLE was calculated from the time-dependent movement of tracer trajectories. Similar to Finite-Size Lyapunov Exponents (FSLE) (Peikert et al., 2014), FTLE calculates areas of potential particle accumulation – including zooplankton – based on the movement of surface currents and has been show to correlate with foraging animal movement patterns (Abrahms et al., 2018; Scales et al., 2014; Scales et al., 2017). A time-series visualization of the FTLE values in the study region was created to assess both the size and temporal persistence of Lagrangian Coherent Structures (LCS), which were visually identified ridges of high FTLE values (Shadden et al., 2005, Video S4). Detailed plots of the regional FTLE values temporally proximal to the observed super-groups were made in R (Version 3.5).

We additionally calculated a time series of surface vorticity in the 6 km x 6 km data cell that encompasses each Monterey super-group (Fig 5B,E) for the period 10-20 Aug 2017. We also calculated surface vorticity in the surrounding study area (25 x 24 cells, Video S5). The raw data were imported and processed in R (Version 3.5) using the ncdf4 package (Version 1.16). Raw surface current data consist of a time vector and two arrays (U and V) representing surface current velocities at each time-step in the eastward (x) and northward (y) directions respectively. Vorticity was calculated as the difference in the derivative of V with respect to x and U with respect to y using the focal function in R Raster package (Version 2.7-15):

$$vorticity = \frac{dV}{dx} - \frac{dU}{dy}.$$

This package utilizes a moving window (e.g. convolution matrix) that passes over each cell and performs an addition of values based on the weights provided in the window to determine a rate of change between neighboring values in a grid. The 3x3 cell convolution matrices used were:

$$x = \begin{bmatrix} -0.25, & 0.00, & 0.25 \\ -0.50, & 0.00, & 0.50 \\ -0.25, & 0.00, & 0.25 \end{bmatrix}, \text{and } y = \begin{bmatrix} 0.25, & 0.50, & 0.25 \\ 0.00, & 0.00, & 0.00 \\ -0.25, & -0.50, & -0.25 \end{bmatrix}.$$

The derivative matrices ($\frac{dV}{dx}$ and $\frac{dU}{dy}$) were combined to calculate vorticity for each grid cell in the time series, resulting in an array of vorticity raster layers of the same dimensions as the original U and V arrays. A time-series visualization of the vorticity in the study region was created to assess both the size and temporal persistence of coherent features over time (Video S5), and the vorticity at each super-group location was plotted over time (Fig 5E).

Sub-surface current data were available near the observed super-groups (M1 in Fig 3A). The RDI/Teledyne Workhorse Long Ranger ADCP at M1 measures water velocity in the upper 500 m. Currents across the depth range of the shelf break (100 – 200 m) were averaged and plotted as a time series (Fig 5F).

In South Africa, oceanographic data were more limited in spatial and temporal resolution. Daily FSLE, similar in their ability to define LCS as FTLE described above (see, e.g.: Abrahms et al., 2018; Scales et al., 2017; Shadden et al., 2005), are an AVISO data product (https://www.aviso.altimetry.fr/en/data/products/value-added-products/fsle-finite-size-lyapunov-exponents.html) calculated following the method of d'Ovidio et al. (2004) at 1/25° x 1/25° spatial resolution. We plotted daily values from -0.2 to 0 in the region where super-groups were observed, from 17.4° to 18.8° E and 32.4° to 34.7°S. We analyzed a 3x3 grid surrounding each observed super-group on its observed day and calculated the minimum FSLE in the grid. We also determined if the grid overlapped with the boundary of an LCS by determining if the grid contained both zero and non-zero FSLE values. For calculating the probability of a randomly chosen point being on an LCS boundary we also determined the boundary status of every point located in the study region in 20-100 m of water.

Aggregation and intake model

To test the likelihood of blue whales independently encountering the high-quality prey patch and aggregating there independently of social information use, we created a simple model comparing random discovery of a prey hotspot to two social cue scenarios using a Monte Carlo simulation with 1000 iterations. Matlab code to construct the model is available at the repository listed in the “data availability” section. In

all models, the habitat was assumed to be the 54 km region of the linear north canyon edge over which we observed blue whales in August 2017 (Fig 3A), whales were assumed to transit the canyon edge at 5.6 km/hr while actively foraging (the mean linear transit speed of the two whales foraging towards the super-group on 16 Aug 2017), the hotspot was assumed to be 2 km long (matching the spatial extent of the observed patch) and located 43 km from the NW edge of the habitat (the approximate location of the second super-group). In all scenarios, once a whale entered the hotspot it would stay there until the end of the simulation. The random foraging model assumed that whales would transit along the canyon edge, but every 10 minutes (approximately the length of a blue whale foraging dive), the whale would randomly move in the same direction or turn back where it came from with equal probability. In the first social cue scenario we assumed that all whales called continuously and that each whale would have a *P*% chance of traveling in the direction where *P*% of the whales were located. In the second social cue scenario, we assumed that whales only called once they were in the hotspot, and that if *P*% of the population were located in the hotspot, individuals had a (50+*P*/2)% chance of turning towards the hotspot. Cumulative intake is the total amount of food consumed by all whales assuming a representative environmental intake rate (λ_{env}) of 1 and a hotspot intake rate (λ_2) of double the environmental rate.

Ethical note

All cetacean data collected under NMFS permits 16111, 20430 and South African permits RES2015/DEA and RES2016/DEA. All procedures were conducted under institutional IACUC protocols. All tagging of wild animals involved non-invasive suction-cup attached tags that detached within 48 hrs. Candidate animals were only chosen if they did not have signs of additional stress (e.g. extreme malnourishment). Tagged animals were monitored upon return to the surface for signs of reactions to tagging, but no unusual behavior was noted. The lowest frequency of our prey-mapping system (38 kHz) was much higher than the threshold of crustacean hearing (which generally have sensitivity peaks < 2 kHz, see Budelmann, 1992), and prior studies have not noted significant differences between quiet vessels

and louder research vessels that would indicate behavioral responses to fisheries acoustics systems in krill (Brierley et al., 2003).

RESULTS

Super-group formation and dispersion

Humpback whale super-groups in South Africa are described in Findlay et al. (2017) and consist of 30-180 whales surfacing in an area as restricted as 100 m on a side (Fig 3D). Super-groups were observed relatively commonly on 10 of 20 ship days in 2015-2016. The precise duration of SG cohesiveness was unknown as none were observed from formation to dispersal, but all were observed for at least 1 hr and were not in the same place the following day. In all five instances where group dispersion was observed in these two observation years, emigration from the group was sequential.

Blue whales were observed and tagged along the Monterey canyon edge from 13-16 Aug 2017. Across the three research vessels, a total of 289 blue whale sightings were recorded, 133 of which were successfully photographed for later identification. Of these 133 photographed encounters, 50 were unique individuals. Applying the known resighting ratio (50/133) to the total sighting record suggests an approximate local population of 109 individuals, so this value was used as our approximate population size in model results. Blue whale abundances of this size are relatively uncommonly reported: small boat surveys in the California Current from 1988 to 2018 encountered at least 25 blue whales in a single day fewer than 6% of the days in which blue whales were sighted (55 out of 963 field days).

Two blue whale super-groups were observed in 2017 (Figs 3,4) and consisted of an estimated 15-40 whales surfacing within sight of an observer at sea level (~ 1 km range). Blue whales are ~ 2x the length and 4x the mass of humpback whales (Kahane-Rapport & Goldbogen, 2018), so we considered the observed blue whale group sizes to be ecologically comparable to the humpback whale super-group sizes. On 14 Aug, the group (25-40 whales estimated) was encountered at 08:30 and had begun to decrease in size at ~11:15. On Aug 16 the group (15-20 whales estimated) was encountered at 13:30 and our vessels left the

area at 14:20. On Aug 15, approximately 8-10 blue whales were feeding in the vicinity of the super-group on Aug 16, but during the Aug 15 encounter, whales were spread out with hundreds of meters separating individuals. Cade et al. (2021) relate how humpback whales and blue whales within super-groups fed at rates 45 and 34 % higher, respectively, compared to feeding rates of whales not in super-groups, and attribute this increase in effort to the less variable distribution of high-quality prey patches within the larger prey patches proximate to super-groups that facilitated shorter transits between high-biomass gulps.

Physical environmental features

Thirty-seven of thirty-nine blue whales were tagged along the Monterey Canyon shelf break along the ~200 m isobath (Fig 3A), a feature known to directly influence ocean circulation and krill distributions (Benoit-Bird et al., 2019; Croll et al., 2005; Santora et al., 2018; Witek, Kalinowski, & Grelowski, 1988). Lunge feeding was predominantly observed above the 200 m bathymetric contour, and both observed blue whale super-group locations were spatially located at krill aggregation hotspots at the heads of narrow, steeply sloping canyons (Fig 4). In South Africa, bathymetric data were of lower resolution but observed aggregations were located near similarly steep features (Fig 3B).

Prey

Super-group associated prey patches were more than two times thicker (mean thickness 33 ± 27 vs 15 ± 15 m in Monterey Bay, 22 ± 14 vs 8 ± 9 m in South Africa), approximately 50% denser, and the denser biomass portions were more evenly distributed than the krill layer along the shelf break (further details in Cade et al., 2021). Super-group associated patches were always found near topographic features (Fig 4). Prey-mapping at the canyon head associated with the super-group observed on 16 Aug was also conducted on 15 Aug. The biomass density measured at the informed whale-scale (the top 50% of gulp-sized cells in the patch) on 15 Aug was 1.87 •⁚ 1.32 kg m^{-3} (-46.5 ± 1.22 dB), where "•⁚" is read "multiplied or divided by" and is the corollary of ± but used to describe the mean and standard deviation of lognormally distributed

biomass in the region of interest (parentheses indicate the raw acoustic units). This was significantly less biomass per gulp-sized cell ($p = 0.039$) with a higher variance than the super-group associated patch on the following day which had a mean biomass density of 2.05 •: 1.26 kg m^{-3} (-46.1 ± 1.0 dB).

Acoustic call detection

Manual audits in MRY for blue whale D calls (Fig 6A, Audio 1), which are thought to be associated with both foraging and aggregations (Miller et al., 2019; Oleson, Calambokidis, et al., 2007), yielded 10,667 detections over 1 Aug 2017 – 15 Sep 2017. The 4-hour bin directly preceding the super-group on 14 Aug had a higher D-call anomaly than 94% of the other 4-hour bins, and the bin preceding the super-group on 16 Aug had a higher anomaly than 97% of bins (Fig 6C). Bars in Fig 6C were colored black if they exceeded the median anomaly + 2 standard deviations, equivalent to the 93rd percentile. The probability that both super-groups would be associated with D-call rates of this magnitude or higher strictly by chance was 0.0049.

Oceanographic features

Temporally, both blue whale super-groups in Monterey Bay were observed when Lagrangian Coherent Structures (LCS) characterized by spatially coherent regions of enhanced FTLE intersected the super-group locations (Fig 5, Video S4). While 24-hr and 96-hr integrations appeared to smooth over super-group associated LCS features (Video S4), both 6-hr and 12-hr integrations predicted enhanced particle aggregation temporally and spatially coincident with both super-group observations. In the 6 km x 6 km region surrounding each super-group location, FTLE cycled on approximately daily cycles, with both super-group observations occurring when local FTLE was at a local maximum.

Both blue whale super-groups also coincided with a boundary between circulation features, specifically the boundary between cyclonic flow over the shelf (blue in Fig 5B) and anticyclonic flow over the slope and deeper offshore waters (red in Fig 5B). Each super-group was observed after periods of

increasing surface vorticity in the 6 km x 6 km analysis region surrounding each super-group location (Fig 5E, Video S5). Offshore (westward) transport at 100-200 m depth at the M1 buoy exhibited local maxima during or immediately preceding the observed super-group events (Fig 5F), indicating an unusually strong flow that may have interacted with the canyon topography.

Ten of eleven observed humpback whale super-groups in South Africa were associated with the edges of LCS (Video S6). The ten groups that did coincide with LCS edges were substantially larger (45-150 estimated whales) than the 06 Nov 2015 group that did not (20 whales). Super-group associated FSLE values ranged from 0 (on 06 Nov 2015) to -0.17, with a mean of -0.08 ± 0.07. Within the identified habitat, the percentage of non-super-group gridded FSLE cells on the boundary of an LCS ranged from 44 to 78% (mean: 63 ± 13 %). The probability that at least ten of eleven randomly chosen points from each day would be on the boundary of an LCS was 0.04, and the probability that all ten large group observations would be on an LCS boundary was 0.01.

Modeling the effects of social cue production

Our random foraging model (Fig 7) predicted that 15 blue whales (our lowest estimate for super-group size) would independently locate the prey hotspot in 3.4 hrs, 25 whales (our median estimate) would take 11.2 hrs, and 40 whales (our high estimate) would take longer than a day. The recruitment rate in the random foraging scenario decreased over time. In the all-calling scenario, recruitment was at first rapid, but then leveled off as the population divided into a SE contingent in the hotspot and a NW contingent that slowly moved towards the hotspot until it was close enough such that an individual 10-minute step would put whales in the hotspot. In the hotspot calling scenario, recruitment rate increased for 13 hrs before declining, and the model predicted that 15 whales would reach the hotspot in 2.3 hrs, 25 whales would arrive in 4.5 hrs, and 40 whales would arrive in 8.0 hrs.

DISCUSSION

Social foraging theory (Giraldeau & Caraco, 2000; Parker & Stuart, 1976) describes two scenarios in which multiple predators exploit a patch of resources (Fig. 1). If the resource is finite and thus depletes faster as the size of the group of foragers increases (i.e. a "dispersion economy"), conditions favor direct competition whereby all foragers would leave the patch nearly simultaneously once the patch is consumed. In such a scenario, and in the absence of some other advantage to maintaining group cohesion, it is to a predator's disadvantage if conspecifics know its location when it finds a high quality patch (Fournet et al., 2018; Page & Bernal, 2020). Echolocating bats, for instance, form large groups of foragers around what are described as "ephemeral" resources (Egert-Berg et al., 2018) and some species have been shown to eavesdrop on the foraging sounds of conspecifics (Page & Bernal, 2020; Roeleke et al., 2020). We use Giraldeau and Caraco's (2000) definition of "ephemeral" to mean not only that the patch is limited in its temporal availability, but also that its quality is driven more strongly by the environment than consumption; that is, the resource declines (or persists) at a rate independent of exploitation. This scenario is particularly relevant for engulfment feeders like rorqual whales, for whom the energetic cost and processing time of each individual foraging event depends on the engulfment volume (Potvin et al., 2020) and will thus be approximately the same regardless of the amount of food in each mouthful, so the packing density of organisms within a swarm can be just as important as overall abundance (Boswell et al., 2016; Burrows et al., 2016; Cade et al., 2021; Hazen et al., 2015).

When resources are locally abundant, as in a prey hotspot, but temporally or spatially ephemeral, Torney et al. (2011) demonstrated that signaling that helps a population track resources can be an evolutionarily stable strategy, even if the recipients are not direct kin and even if signaling has a cost (directly or indirectly through competitive exclusion). If both the direct and indirect costs of signaling are low, it would imply that information sharing would be even more strongly selected for. We thus propose that a predator-prey system characterized by extensive, ephemeral, environmentally controlled prey patches exploited by predators with low costs of transport and the ability to produce social cues detectable over

large distances would be expected to utilize an information sharing strategy to increase environmental information and avoid the pitfalls associated with finding patches individually (Hein & Martin, 2020; Wilson et al., 2018). We propose four reasons that this scenario characterizes rorqual whale super-groups.

Extensive, ephemeral, environmentally controlled prey patches

The patches we observed coincident with super-groups contained more biomass than could be consumed by the observed whales over relevant time scales. The densest 50% of gulp-sized cells (the "informed whale-scale" described in Cade et al., 2021) in the measured portion of the super-group associated prey patch from 16 Aug 2017 (SG B in Fig 4), which is only a slice of the overall patch, were echo returns from organisms in 1.1 million m^3 of water (accounting for overlap between pings). This slice alone would take 40 blue whales nine hours to consume at their super-group feeding rates. Additionally, Cade et al. (2021) showed that super-group associated prey patches were not only higher in biomass (higher λ_ρ, Fig 2), but also were distributed in such a way as to increase foraging rates (λ_f), resulting in an overall higher patch quality (λ) than nearby krill layers in which whales were also observed foraging prior to or subsequently to super-group observations.

Secondly, although the sizes of super-group associated prey patches exceeded one km, the highest quality areas were spatially restricted by topographically constrictive bathymetric features (Figs 3 & 4). Monterey Canyon, the largest submarine canyon along the US west coast, is known to be a krill hotspot and essential foraging habitat for blue whales (Croll et al., 2005; Santora et al., 2012; Schoenherr, 1991). Submarine canyons and other physical features such as island wake eddies (Johnston et al., 2005), tidal flow (Cotté & Simard, 2005), and internal waves (Hazen et al., 2009; Pineda et al., 2015) can create prey-aggregation hot-spots on hourly-daily timescales by disrupting flow patterns and creating hydrodynamic structures that advect, entrain or attract freely swimming micronekton to local areas (S. Allen et al., 2001; Benoit-Bird et al., 2019; Santora et al., 2018). These fine-scale ocean features have been shown to be associated with prey aggregations and, in turn, result in increased predator foraging opportunities. Our observations of both blue whale super-groups at the heads of small canyons incising the slope support the

importance of canyons and flow-topography interactions and imply that the observed spatially restricted blue whale aggregations were related to the spatial scale of prey aggregations.

Thirdly, physical oceanographic features aligned spatially and temporally with observed krill patches and blue whale super-groups. Krill are known to aggregate along oceanographic barriers and near submarine canyons like the ones we observed near super-groups (Santora et al., 2018; Warren & Demer, 2010) but to become more diffuse in the absence of strong circulatory patterns like upwelling that often act on sub-daily timescales in relation to diel wind patterns and semi-diurnal tides (Benoit-Bird et al., 2019; Johnston et al., 2005). Specifically, areas where currents form features that interact with one another, such as fronts, jets, or eddies, have been linked to animal habitat selection in multiple systems (Abrahms et al., 2019; Oliver et al., 2019) due to their potential to aggregate biomass (Abrahms et al., 2018; Scales et al., 2014). In South Africa, observed super-groups were associated with the boundaries of LCS, and in 2016 a strong feature (mean FSLE < -0.1) formed outside of Saldanha Bay (Fig 3B ii, Video S6) that was not present in 2015 when no aggregations were observed there. In Monterey Bay, water velocity across the shelf break depth range at the M1 buoy indicated circulation patterns that may have influenced foraging conditions, as super-group encounters coincided with two periods of high current speeds in the shelf break depth range: strong northward flow during and preceding each super-group observation (Fig 5F) may have accumulated krill swarms while transporting them on-shelf along the upward-sloping seafloor, while sharp pulses of strong westward flow may have rapidly ejected near-bottom krill swarms into the shelf break water column, transporting them seaward into deeper water. Both blue whale super-group encounters were temporally coincident with observable surface FTLE and vorticity features that persisted on the scale of hours and were not present one week prior or one week past when the aggregations were observed (Fig 5, Videos S4&S5), suggesting that the size and density of the observed prey patches were environmentally influenced. Observations of the prey patch associated with super-group B over two successive days (Fig 4 C&D) support these interpretations. On 15 Aug when the patch was large in size but not as uniformly dense as the super-group associated patch on 16 Aug, there were 8-10 blue whales feeding in the area with 100s of m of separating them (i.e., not aggregated into a super-group). It should be noted that the surface features

intersecting the canyon edge were also observable at other times during the study period, but it is not known whether large prey patches, and large predator aggregations, formed at those times in those locations. Future studies will be needed to more closely link the prey field along the shelf break to surface features.

Finally, we also found evidence that super-group formation may be socially-mediated. Rorqual whales forage across large expanses of the ocean, a consummate acoustic medium (Au & Hastings, 2008), and their low-frequency vocalizations can be perceived over tens to hundreds of kilometers (Stafford et al., 1998). We recorded anomalously high rates (> 94th percentile) of D calls – thought to be associated with foraging behavior in blue whales (Barlow et al., 2021; Miller et al., 2019; Oleson, Calambokidis, et al., 2007) – at the MARS hydrophone in the four-hour bins preceding both observations of super-groups in Monterey Bay, suggesting that blue whales may increase calling activity near high-quality foraging grounds. Anomalously high D call production was also recorded in subsequent days (17 & 18 Aug), and although field efforts had concluded (so aggregations could not be confirmed), high-magnitude LCS continued to form around the Monterey Canyon edge over the same time period (Video S4), suggesting that conditions for super-patch creation remained in place through the period of observed anomalously high social cue production. Modeled results (Fig 7) demonstrate that the observed blue whale group sizes, which were likely more than 25 and as high as 40 animals, formed much more rapidly if social information informed travel direction. The increase in cumulative resource intake in the population that was assumed to use social information provides additional evidence of a benefit that could result in an evolutionarily stable foraging strategy. Our observations during the study period support these models: two blue whales tagged prior to the 16 Aug super-group both traversed along the shelf break and joined the forming aggregation (Video S7), suggesting knowledge about the environment that presumably exceeded their sensory perception (as modeled in Fig 8D). Although we did not have equivalent recordings in South Africa, prior studies found evidence of song production near super-groups (Gridley et al., 2018; Ross-Marsh et al., 2020). Though it is more typically associated with breeding grounds, song is among the loudest humpback whale vocalizations. This contrasts with other regions characterized by foraging on depletable fish schools,

like SE Alaska, where humpback whale vocalizations have been noted to be quieter than expected (Fournet et al., 2018), likely to avoid alerting conspecifics.

The implications of the environmentally-controlled social foraging scenario we propose are modeled in Fig 8. In these models, we propose that the mean intake rate for any individual (λ) – for modeling purposes equivalent to the environmental patch quality that facilitates an individual's intake rate (Giraldeau & Caraco, 2000) – can be described by $\lambda = \lambda_0 \varepsilon^t$, where ε represents the environmental input such that the patch declines if $\varepsilon < 1$, stays constant at $\varepsilon = 1$ and grows if $\varepsilon > 1$, where λ_0 is the initial intake rate and t is time. The plots show cumulative intake of an individual over time, such that the slope of the line at any point is the intake rate λ. The scenarios described differ from the ephemeral prey patch model in Giraldeau and Caraco (2000) in that they do not assume that the intake of a solitary forager differs from that of a forager in a group. They also allow both for search/exploitation cycle durations that vary and for λ that remain steady within a patch for some non-trivial period of time. In order to effectively characterize the environment in which krill-feeding rorqual whales forage, the environmentally-controlled, ephemeral, non-competitive social foraging scenario we propose rests on four assumptions that could be tested in systems that have exhibit similar environmental characteristics: 1) calling rates of foraging individuals increase as prey density increases (supporting the prediction of the "hotspot calling" scenario in Fig 7), 2) high calling rates in an environment increase the probability that an individual gives up foraging to transit to a distant patch, 3) individuals will emigrate from a patch being exploited as a group once quality declines below their individually determined mean intake rate (as discussed in Fig 2), 4) larger animals will leave a patch first as quality declines since their intake rate will be more dependent on closely spaced, dense patches (Kahane-Rapport et al., 2020). If these hypotheses can be verified in future research, it will have implications for search and exploitation times of rorqual whales, their dependence on conspecifics to extend their sensory perception, and their resilience to annual fluctuations in the environment.

Conclusions

The gigantic body sizes characteristic of rorqual whales not only increase the efficiency of foraging on krill (Goldbogen et al., 2019), but also appear to enable some of the foraging flexibility of species like humpback whales (Cade et al., 2020). It was not until relatively recently in the fossil record (5-7 Ma) that baleen whales developed gigantic body sizes (> 10 m), and it is likely that this large change came about in concert with oceanic conditions that favored annually consistent upwelling zones that brought nutrient-rich water to the surface in specific areas, stimulating primary productivity and promoting natural aggregation areas (Slater, Goldbogen, & Pyenson, 2017). Locating and exploiting prey hotspots is essential to the foraging strategy of rorqual whales, but whale aggregations of the size and density noted here are not commonly reported. In the case of humpback whales, groups of the size and density discussed here have only been reported in South Africa seasonally and recently (Findlay et al., 2017), and have also only recently been observed during the southward migration in Australia (Pirotta et al., 2021). However, similarly large aggregations of rorqual whales were reported historically (e.g. Bruce, 1915) and the contemporary reemergence of this behavior may be related to the recovery of regional large whale populations above critical thresholds, especially given that abnormally large densities of krill do not appear to be a new phenomenon (Nicol, James, & Pitcher, 1987).

The historic reports and contemporary reemergence of these large aggregations suggest that social cues emanating from super-groups may have played an important role as signposts to help individuals in a population more purposefully navigate patchy environments (Wilson et al., 2018), essentially improving their foraging success by extending their sensory capabilities (Hein & Martin, 2020; LaScala-Gruenewald et al., 2019). The 19th and 20th century commercial exploitation of all large cetaceans would therefore have led to massive information network disruption (Schmidt, Dall, & Van Gils, 2010) as populations plummeted to numbers that were between 1-10% of historic abundance. However, if large populations of rorqual whales can increase their foraging efficacy by revealing the location of high-quality foraging hotspots to conspecifics, the resulting positive feedback loop may help explain why large whale populations were slow

to recover from 19th and 20th century commercial exploitation, but some populations have more recently increased in abundance (Bejder et al., 2016). In contrast, some exploited, particulate-feeding species such as sperm whales have recovered more slowly than expected (Carroll et al., 2014; Gero & Whitehead, 2016).

Both the propensity to form large groups and the types of collective behavior are strongly driven across taxa by the heterogeneity, or patchiness, of resources in the environment (Gordon, 2014; Piatt & Methven, 1992). Resource dispersion hypotheses posit that heterogeneous (patchy) environments increase the degree to which living in groups is an evolutionarily stable strategy (Torney et al., 2011), but there are few systems in which these hypotheses have been explicitly tested (Johnson et al., 2002). Due to the variety of rorqual whale group sizes, as well as the newly developed ability of researchers to study these groups quantitatively in the wild (Goldbogen et al., 2013), we propose these groups are ideal systems in which to test a variety of theories related to social foraging. There is growing evidence that individual behavior influences social foraging dynamics (Laskowski & Bell, 2014), but also that environmental variability influences individual behavior (Araújo, Bolnick, & Layman, 2011). As large, long-lived, individually identifiable organisms, rorqual whale behavior can be studied longitudinally, allowing the spreads of behaviors within populations to be studied quantitatively (J. Allen et al., 2013), and future research may be able to answer the open question of the degree to which individual rorqual whales can adjust their foraging strategies to environmental regimes that are increasingly dynamic. It may be that as a consequence of its dynamic patchiness, the marine environment encourages more cooperative dynamics generally than the terrestrial realm.

Figures

(following pages)

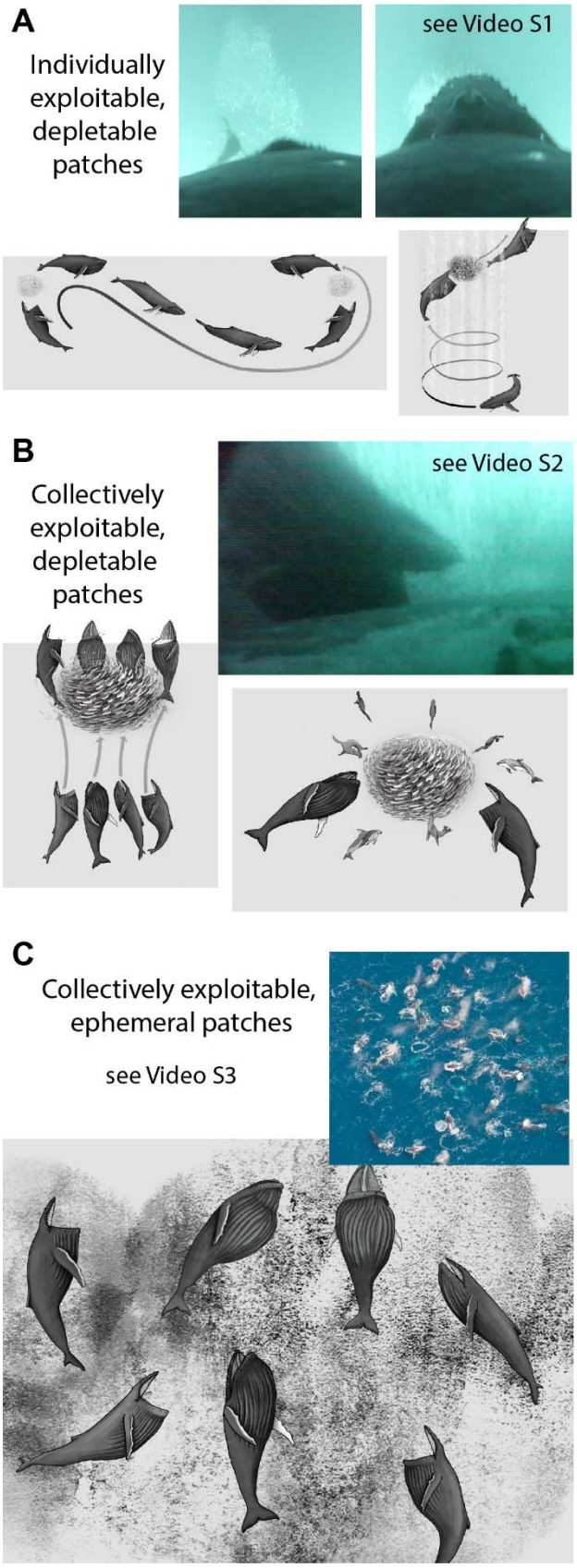

Fig 1- Social patch and prey models (Giraldeau & Caraco, 2000) in humpback whale predator-prey systems. A) Individually exploitable, depletable patches that are consumed after a single gulp by an individual whale. Images are from an animal-attached camera on a humpback whale approaching an anchovy school in the Santa Barbara Channel, USA. Drawings are schematics of a humpback whale foraging on krill schools and an individual whale blowing a bubble net to herd herring or sand lance. B) Collectively exploitable, depletable patches. These fish schools are larger and break apart easily. They generally are kept together either by multiple species of predators or by groups of humpback whales blowing bubbles and then lunging synchronously through the school. C) Collectively exploitable, ephemeral patches. "Ephemeral" in this context, means the patch size is so large that it is not meaningfully depleted by foraging whales, but its diminishment is environmentally controlled. UAV image © Jean Tresfon, illustrations by Alex Boersma.

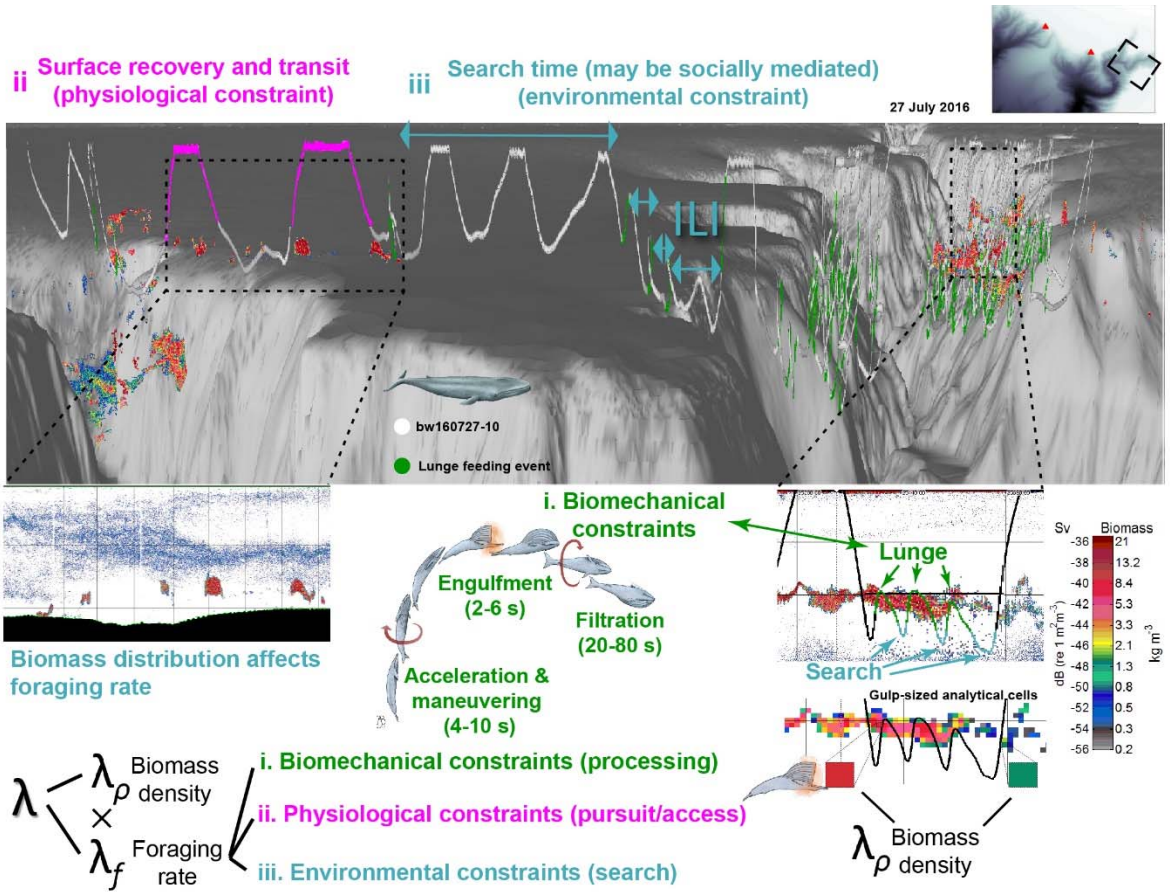

Fig 2- As a modelling parameter, λ links the patch quality to a predator's intake rate. In rorqual whales, the environment is represented by krill biomass and distribution, which affects the transit time between lunge-feeding events such that it controls both λ_ρ and λ_f. λ_f may also be influenced by social information that decreases patch detection time. Foraging rate is also a result of individual parameters including biomechanical and physiological constraints such that larger animals spend a larger portion of their foraging time processing food (Kahane-Rapport et al., 2020). Three-dimensional plot crafted in Echoview v 10 using a 10x vertical exageration and 120 kHz data, with the spatially matched track of a tagged blue whale. Biomass estimated as in (Cade et al., 2021). Two-dimensional plots are temporally linked echosounding data with the tagged whale's depth profile. Illustrations by Alex Boersma.

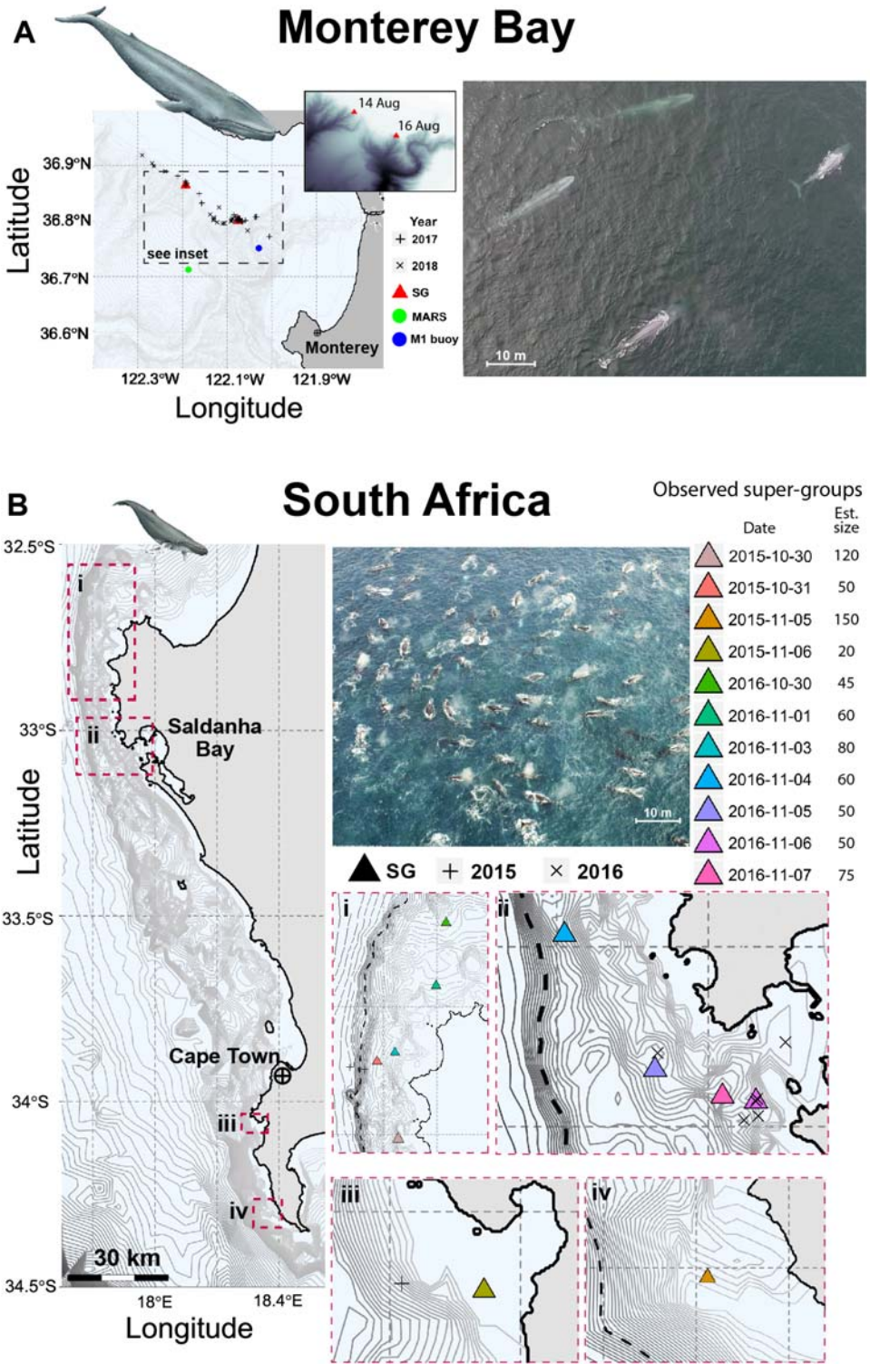

Fig 3- Super-group locations in each study area. Triangles show observed super-group (SG) locations, and + and × mark the deployment locations of suction-attached bio-loggers A) In Monterey Bay, blue whale super-groups were observed at the heads of small slope-incising canyons (see also Fig 4). UAV image is from super-group B on 16 Aug 2017, image © Duke Marine Robotics and Remote Sensing. Depth contour lines are separated by 50 m. B) In South Africa, super-groups were found associated with complex bathymetry. Depth contour lines are separated by 3 m from 30 m to 120 m, then 10 m thereafter. Dotted line in insets is the 99 m isobath. UAV image © Dave Hurwitz

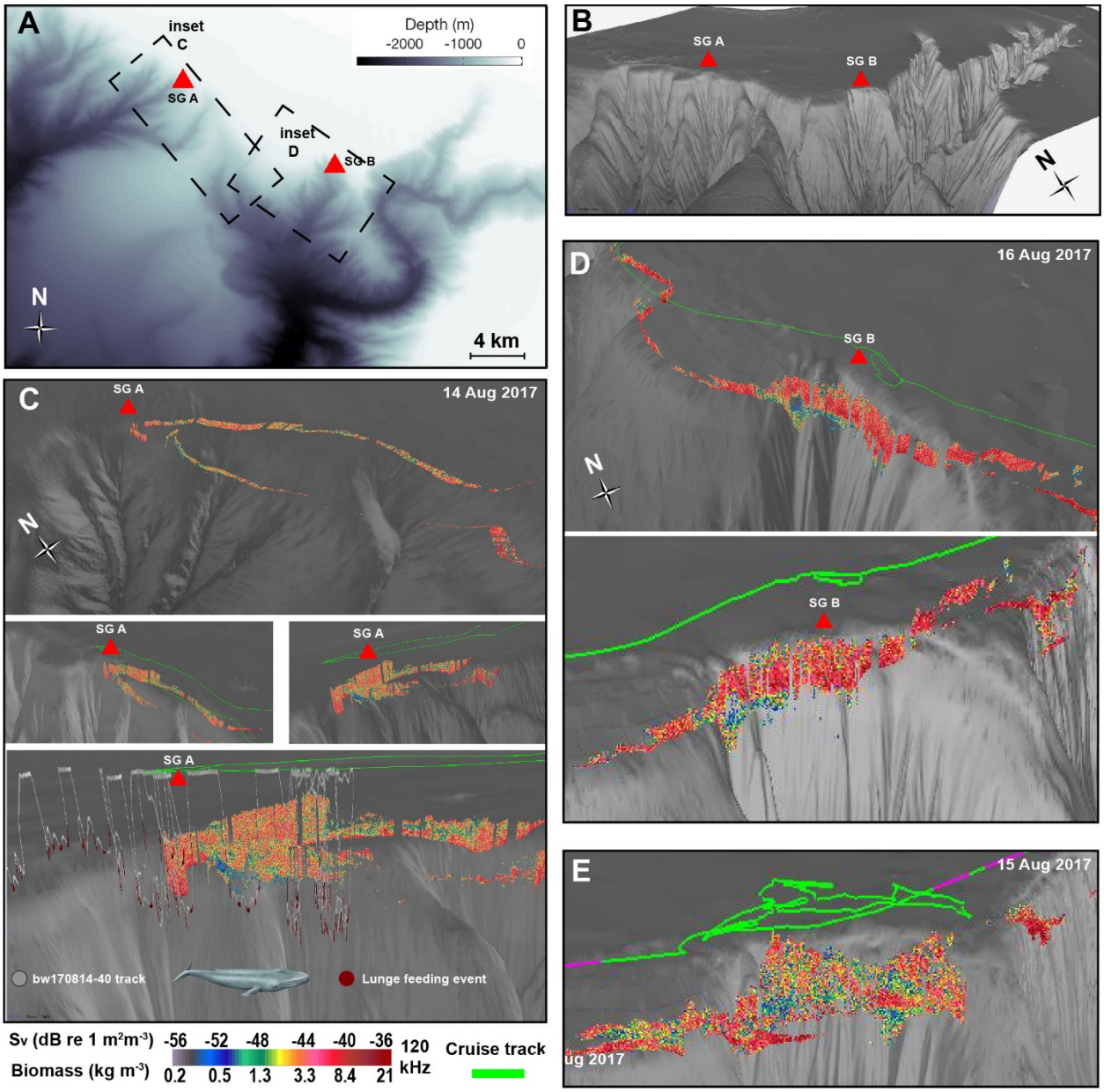

Fig 4- Topographic context of observed blue whale super-groups (SG) and SG-associated prey patches. A) General bathymetry of Monterey Canyons, SG A (25-40 whales) was observed on 14 Aug 2017 and SG B on 16 Aug 2017 (15-20 whales). B) 3D plot of Monterey Canyon. C) Several views of the prey field around SG A. Bottom panel includes the track of tagged whale bw170814-40 showing concentrated foraging at the heads of small narrow canyons. D) Two views of SG B. E) Comparison plot of the prey field in the same location as SG B but one day earlier. All 3D plots crafted in Echoview v10 using a 10x vertical exageration.

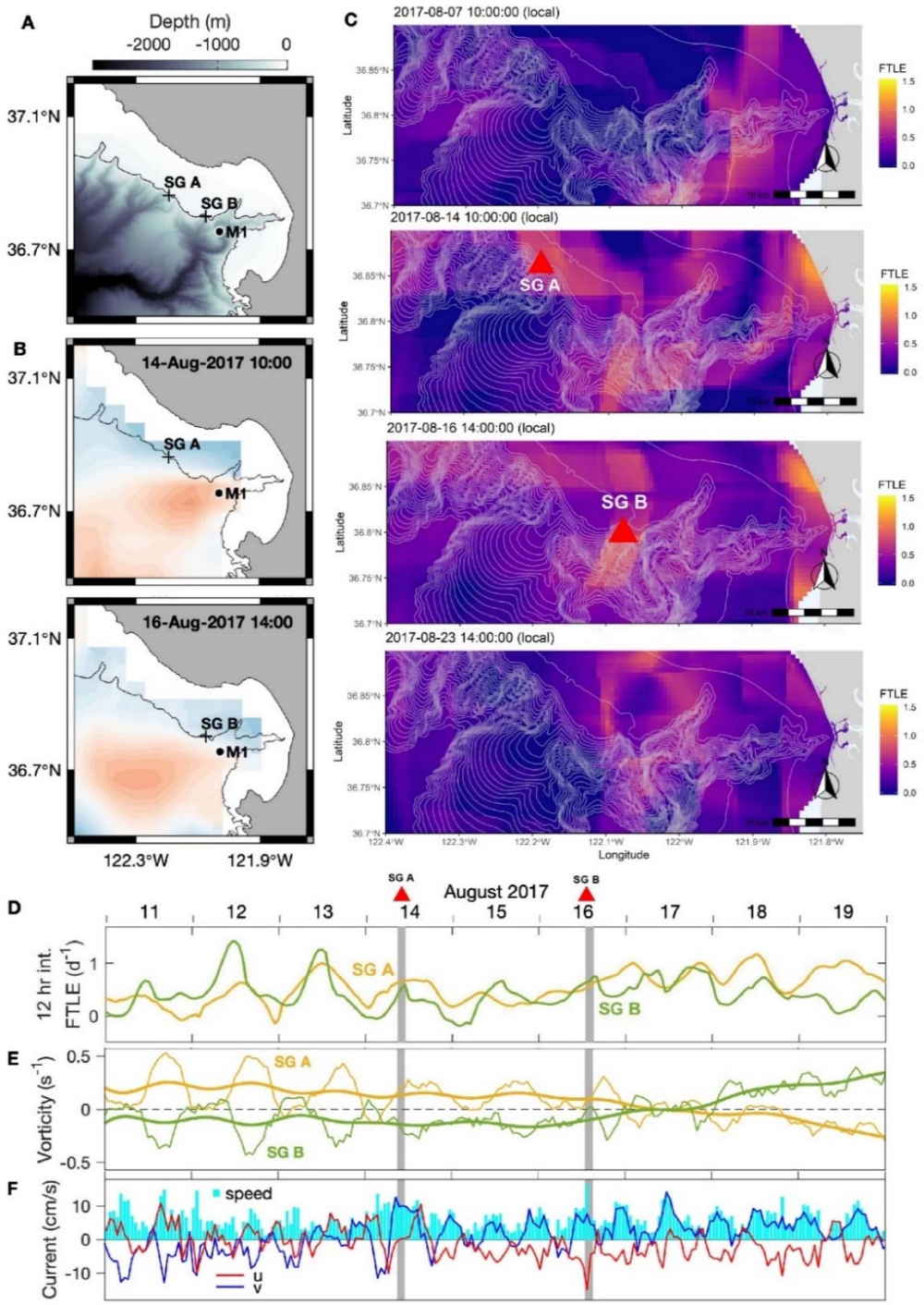

Fig 5- Oceanographic processes interacting with topography. A) High-resolution bathymetry map; overlaid are the 200 m isobath, locations of super-group (SG) encounter, and the location of environmental mooring M1 (36.755°N, 122.03°W; 18.9 and 6.4 km from the super-group observation locations. B) Vorticity maps coincident with each super-group encounter. Boundaries between surface vorticity features could indicate a sub-surface front known to aggregate prey. C) Selected spatial maps of 12 hr backwards-in-time integrated FTLE values one week before the first SG encounter, at the times of each SG, and one week after the second SG. FTLE is a metric of simulated particle aggregation based on measured surface currents. D&E) Time-series of FTLE and vorticity, respectively of the grid cell containing the observed super-group; thick lines in E are 33-hour low-pass filtered. F) Time series of average currents in the depth range 100 – 200 m at the M1 mooring.

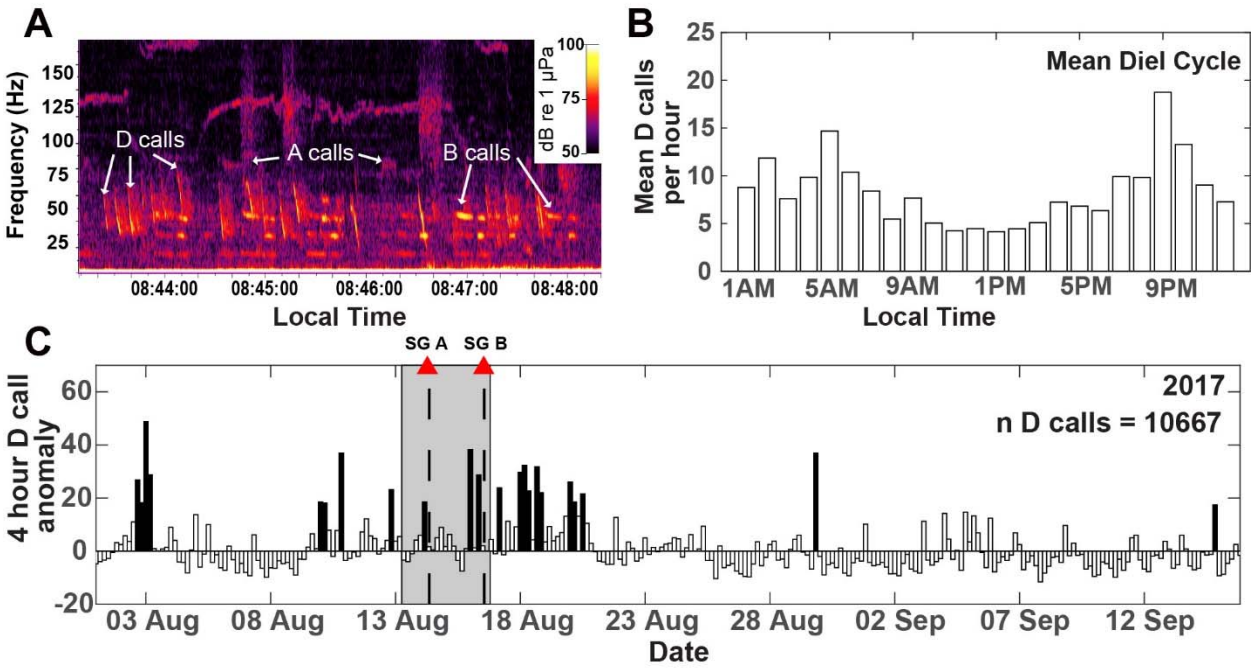

Fig 6- Blue whale D calls recorded during the 2017 field season at the MARS hydrophone. A) Spectrogram display (FFT parameters: Hann window, 1024 samples, 95% overlap, Raven Pro v1.5) of passive acoustic data from 16 Aug 2017. Northeast Pacific blue whale D calls are prevalent, and A and B calls are also labeled. B) Mean diel cycle of D call counts over August 1st – September 15th of 2017 and 2018. C) Time series of 2017 4-hour D call anomalies (defined as the number of calls above or below the mean diel value for that 4-hour bin). Dark bars indicate outlier 4-hour periods exceeding the median anomaly by more than two standard deviations. Dashed lines and red triangles indicate the times of observed blue whale super-groups (SG). Shading indicates field effort during 2017.

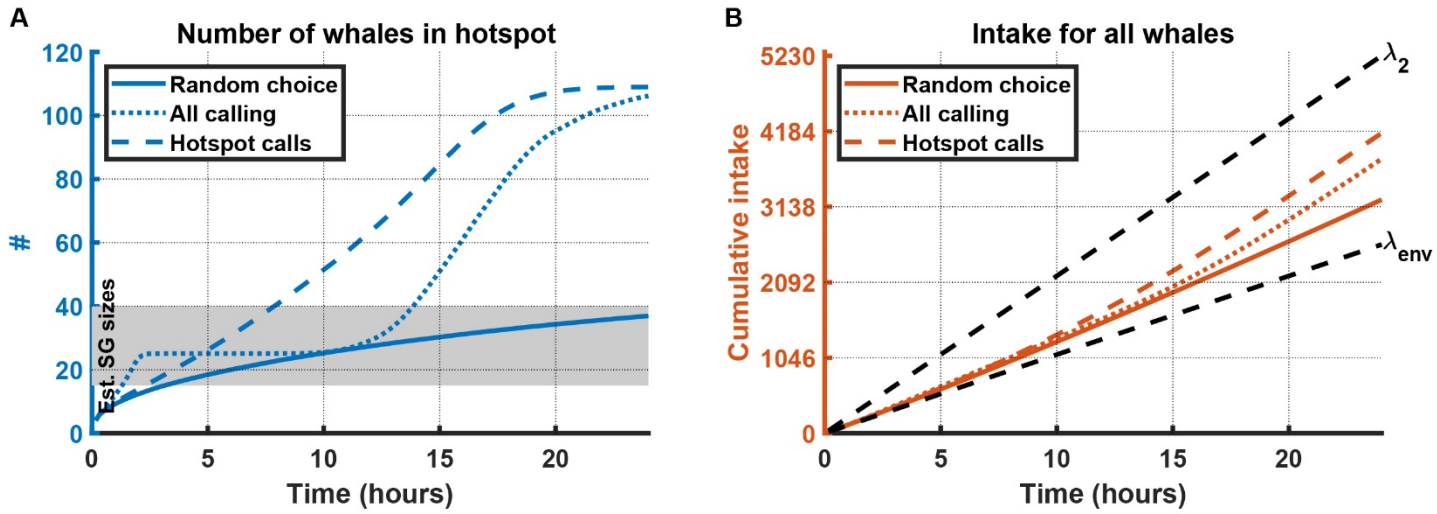

Fig 7- Simple model results from 1000 trials given random foraging or two social information scenarios predicting A) the number of whales to find a prey hotspot and B) the cumulative intake of all whales. λ_{env} is a representative intake rate, while λ_2 is the representative hotspot intake rate.

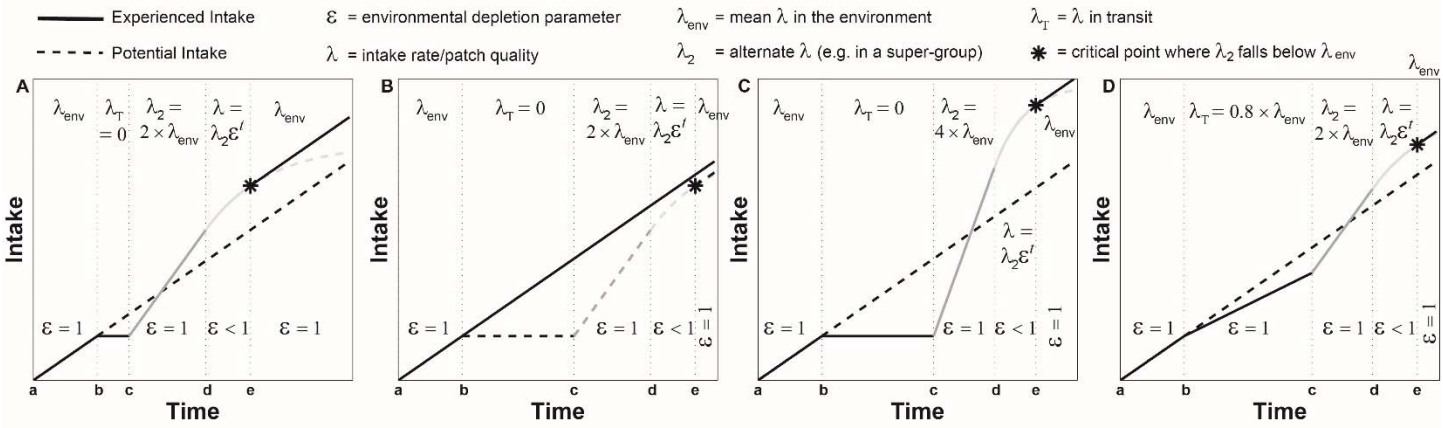

Fig 8- A model of resource intake in an environmentally-controlled, ephemeral, non-competitive social foraging scenario. In all panels, y-axis is cumulative intake, x-axis is time (t), and λ, the intake rate, is the slope at any given time *t*. The time steps are: a) animal foraging with an environmentally influenced intake rate λ_{env}, b) animal detects conspecific cues and either continues foraging or breaks off foraging to transit to the conspecific aggregation, c) animal arrives at aggregation and begins foraging at λ_2, the new intake rate, d) the intake rate at the patch begins to decline as a result of environmental controls until e) the point when the slope of the intake function reaches λ_{env}, and the forager is motivated to leave the patch. Panel (A) represents an animal foraging at λ_{env} when it detects a cue and transits without feeding to the source, the increased intake rate results in a higher overall intake than if the individual had stayed in its original environment. B) an animal detects a similar aggregation, but its distance is far enough such that increased foraging would not make up for the loss of intake during transit, in this scenario the optimal foraging strategy is not to transit. C) A forager detects cues the same distance as the prior scenario, but the strength of the cues (e.g. calling rate) is such that it implies that λ_2 would be high enough to account for the long transit time D) When prey are arranged in long layers, as in along a shelf break, it could be optimal to continue foraging but towards the direction of the cue source such that transit is longer but overall intake is still higher. This appears to be what we observed with two tagged blue whales that fed along the shelf break to the SE towards the direction of super-group B (Video S7).

Supporting Information

Video S1- A humpback whale (tag ID# mn170809-41) foraging on individually-exploitable, depleteable patches of anchovies

Video S2- A humpback whale in California (tag ID# mn181002-45) foraging on a large, collectively-exploitable, depletable patch of anchovies in a multi-species aggregation. The first lunge attempt was interrupted by conspecifics. Corner animation based on scripts from animaltags.org.

Video S3- A humpback whale in South Africa (tag ID# mn161105-37) feeds apparently non-competitively within an extensive prey patch whose depletion is likely independent of foraging effort.

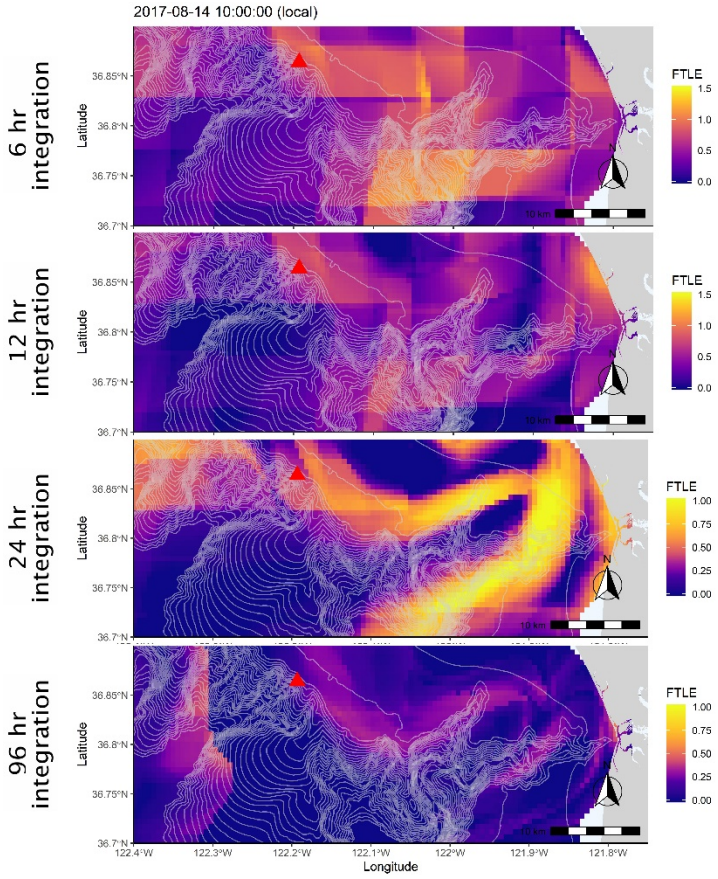

Video S4- Time series of FTLE features around Monterey super-group formations with four backwards-in-time integration durations displayed simultaneously. Lagrangian coherent structures (LCS) are apaprent at all four integration scales, and 6-12 hr integration periods result in LCS that most readily spatially and temporally match the super-group predator and prey observations.

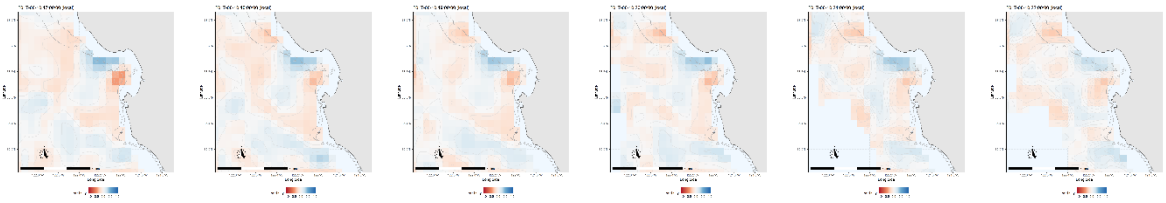

Video S5- Time series of vorticity features around Monterey super-group formations.

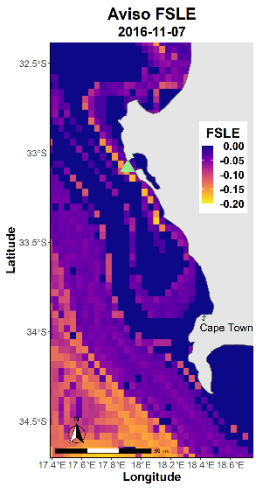

Video S6- Time series of FSLE features around observed South Africa super-groups

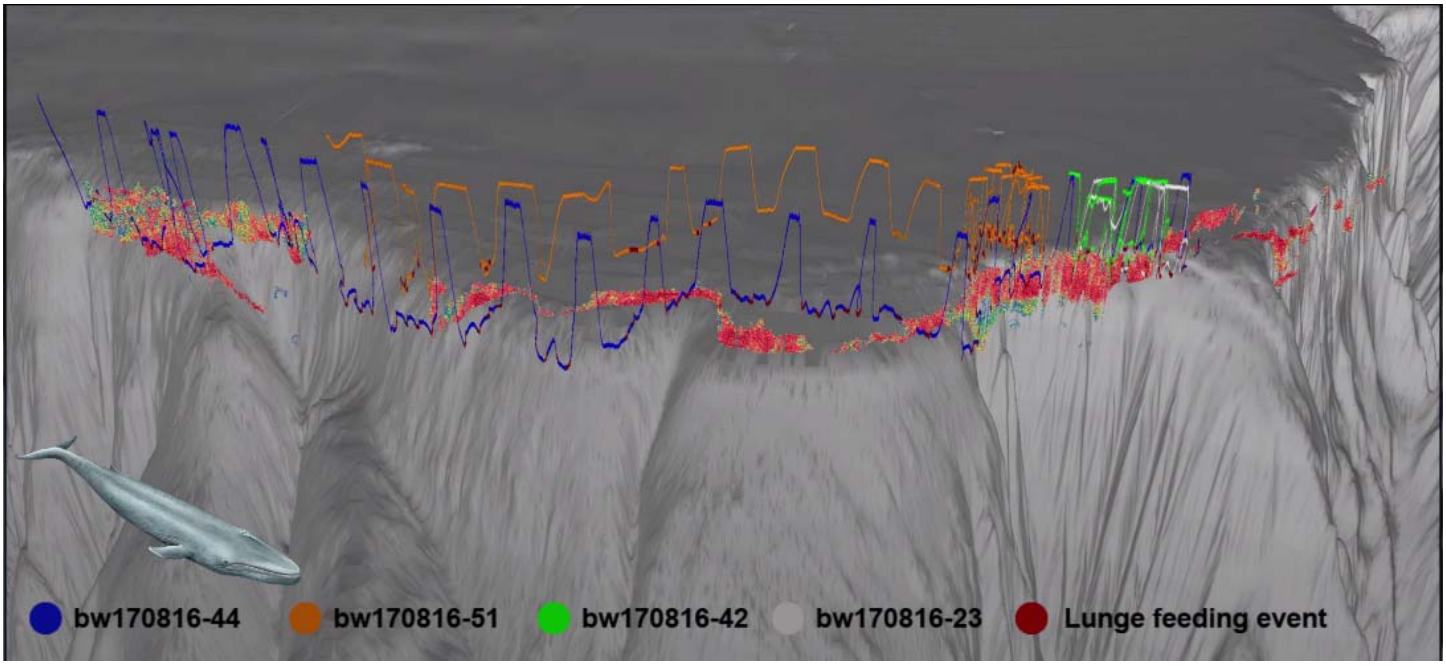

Video S7- Time series of tagged blue whales approaching the super-group location on 16 Aug 2017.

Audio S1- A NE Pacific blue whale D call as recorded on the MARS hydrophone

DATA AVAILABILITY

Code to create Fig 7 as well as prey and tag data have been deposited at Stanford University's digital repository: https://purl.stanford.edu/rq794kc6747, MARS hydrophone data can be accessed at: https://www.mbari.org/at-sea/cabled-observatory/mars-science-experiments/mars-hydrophone-data/, surface current data (used to derive vorticity and particle accumulation) is publicly available at: http://www.sccoos.org/data/hfrnet/, and M1 current data is available through: https://www.cencoos.org/data/buoys/mbari/m1/info

REFERENCES

Abrahms, B., Hazen, E. L., Aikens, E. O., Savoca, M. S., Goldbogen, J. A., Bograd, S. J., . . . Mate, B. R. (2019). Memory and resource tracking drive blue whale migrations. *Proceedings of the National Academy of Sciences, 116*(12), 5582-5587.

Abrahms, B., Scales, K. L., Hazen, E. L., Bograd, S. J., Schick, R. S., Robinson, P. W., & Costa, D. P. (2018). Mesoscale activity facilitates energy gain in a top predator. *Proceedings of the Royal Society B: Biological Sciences, 285*(1885), 20181101.

Allen, J., Weinrich, M., Hoppitt, W., & Rendell, L. (2013). Network-based diffusion analysis reveals cultural transmission of lobtail feeding in humpback whales. *Science, 340*(6131), 485-488.

Allen, S., Vindeirinho, C., Thomson, R., Foreman, M. G., & Mackas, D. (2001). Physical and biological processes over a submarine canyon during an upwelling event. *Canadian Journal of Fisheries and Aquatic Sciences, 58*(4), 671-684.

Ameli, S., & Shadden, S. C. (2019). A transport method for restoring incomplete ocean current measurements. *Journal of Geophysical Research: Oceans, 124*(1), 227-242.

Araújo, M. S., Bolnick, D. I., & Layman, C. A. (2011). The ecological causes of individual specialisation. *Ecology letters, 14*(9), 948-958.

Au, W. W., & Hastings, M. C. (2008). *Principles of marine bioacoustics*: Springer.

Baines, M., Reichelt, M., & Griffin, D. (2017). An autumn aggregation of fin (*Balaenoptera physalus*) and blue whales (*B. musculus*) in the Porcupine Seabight, southwest of Ireland. *Deep Sea Research Part II: Topical Studies in Oceanography, 141*, 168-177.

Barange, M. (1994). Acoustic identification, classification and structure of biological patchiness on the edge of the Agulhas Bank and its relation to frontal features. *South African Journal of marine science, 14*(1), 333-347.

Barlow, D. R., Klinck, H., Ponirakis, D., Garvey, C., & Torres, L. G. (2021). Temporal and spatial lags between wind, coastal upwelling, and blue whale occurrence. *Scientific reports, 11*(1), 1-10.

Becker, E. A., Forney, K. A., Foley, D. G., Smith, R. C., Moore, T. J., & Barlow, J. (2014). Predicting seasonal density patterns of California cetaceans based on habitat models. *Endangered Species Research, 23*(1), 1-22.

Bejder, M., Johnston, D. W., Smith, J., Friedlaender, A., & Bejder, L. (2016). Embracing conservation success of recovering humpback whale populations: evaluating the case for downlisting their conservation status in Australia. *Marine Policy, 66*, 137-141.

Benoit-Bird, K. J., & McManus, M. A. (2012). Bottom-up regulation of a pelagic community through spatial aggregations. *Biology Letters, 8*(5), 813-816.

Benoit-Bird, K. J., Waluk, C. M., & Ryan, J. P. (2019). Forage Species Swarm in Response to Coastal Upwelling. *Geophysical Research Letters, 46*(3), 1537-1546.

Bernstein, C., Kacelnik, A., & Krebs, J. R. (1991). Individual decisions and the distribution of predators in a patchy environment. II. The influence of travel costs and structure of the environment. *The Journal of Animal Ecology*, 205-225.

Blukacz, E., Shuter, B., & Sprulesc, W. (2009). Towards understanding the relationship between wind conditions and plankton patchiness. *Limnology and Oceanography, 54*(5), 1530-1540.

Boswell, K. M., Rieucau, G., Vollenweider, J. J., Moran, J. R., Heintz, R. A., Blackburn, J. K., & Csepp, D. J. (2016). Are spatial and temporal patterns in Lynn Canal overwintering Pacific herring related to top predator activity? *Canadian Journal of Fisheries and Aquatic Sciences, 73*(999), 1-12.

Brierley, A. S., Fernandes, P. G., Brandon, M. A., Armstrong, F., Millard, N. W., McPhail, S. D., . . . Squires, M. (2003). An investigation of avoidance by Antarctic krill of RRS James Clark Ross using the Autosub-2 autonomous underwater vehicle. *Fisheries Research, 60*(2-3), 569-576.

Brown, C. R. (1988). Social foraging in cliff swallows: local enhancement, risk sensitivity, competition and the avoidance of predators. *Animal Behaviour, 36*(3), 780-792.

Bruce, W. (1915). Some observations on Antarctic cetacea. *Scotia Natl. Antarct. Exped. Rep, 4*, 491-505.

Buckley, N. J. (1997). Spatial-concentration effects and the importance of local enhancement in the evolution of colonial breeding in seabirds. *The american naturalist, 149*(6), 1091-1112.

Budelmann, B. U. (1992). Hearing in crustacea *The evolutionary biology of hearing* (pp. 131-139): Springer.

Burrows, J. A., Johnston, D. W., Straley, J. M., Chenoweth, E. M., Ware, C., Curtice, C., . . . Friedlaender, A. S. (2016). Prey density and depth affect the fine-scale foraging behavior of humpback whales Megaptera novaeangliae in Sitka Sound, Alaska, USA. *Marine Ecology Progress Series, 561*, 245-260.

Cade, D. E., Carey, N., Domenici, P., Potvin, J., & Goldbogen, J. A. (2020). Predator-informed looming stimulus experiments reveal how large filter feeding whales capture highly maneuverable forage fish. *Proceedings of the National Academy of Sciences, 117*(1), 472-478.

Cade, D. E., Seakamela, S. M., Findlay, K. P., Fukunaga, J., Kahane-Rapport, S. R., Warren, J. D., . . . Goldbogen, J. A. (2021). Predator-scale spatial analysis of intra-patch prey distribution reveals the energetic drivers of rorqual whale super group formation. *Functional Ecology, 35*(4), 894-908. doi: 10.1111/1365-2435.13763, http://dx.doi.org/10.1111/1365-2435.13763

Carroll, G., Hedley, S., Bannister, J., Ensor, P., & Harcourt, R. (2014). No evidence for recovery in the population of sperm whale bulls off Western Australia, 30 years post-whaling. *Endangered Species Research, 24*(1), 33-43.

Chapman, R., Shay, L. K., Graber, H. C., Edson, J., Karachintsev, A., Trump, C., & Ross, D. (1997). On the accuracy of HF radar surface current measurements: Intercomparisons with ship-based sensors. *Journal of Geophysical Research: Oceans, 102*(C8), 18737-18748.

Clark, K. L., & Robertson, R. J. (1979). Spatial and temporal multi-species nesting aggregations in birds as anti-parasite and anti-predator defenses. *Behavioral Ecology and Sociobiology, 5*(4), 359-371.

Coetzee, J. (2000). Use of a shoal analysis and patch estimation system (SHAPES) to characterise sardine schools. *Aquatic Living Resources, 13*(1), 1-10.

Cotté, C., & Simard, Y. (2005). Formation of dense krill patches under tidal forcing at whale feeding hot spots in the St. Lawrence Estuary. *Marine Ecology Progress Series, 288*, 199-210.

Croll, D. A., Marinovic, B., Benson, S., Chavez, F. P., Black, N., Ternullo, R., & Tershy, B. R. (2005). From wind to whales: trophic links in a coastal upwelling system. *Marine Ecology Progress Series, 289*, 117-130.

d'Ovidio, F., Fernández, V., Hernández-García, E., & López, C. (2004). Mixing structures in the Mediterranean Sea from finite-size Lyapunov exponents. *Geophysical Research Letters, 31*(17).

Dodson, S., Abrahms, B., Bograd, S. J., Fiechter, J., & Hazen, E. L. (2020). Disentangling the biotic and abiotic drivers of emergent migratory behavior using individual-based models. *Ecological Modelling, 432*, 109225.

Dunlop, R. A., Cato, D. H., & Noad, M. J. (2008). Non-song acoustic communication in migrating humpback whales (Megaptera novaeangliae). *Marine Mammal Science, 24*(3), 613-629.

Dustan, P., & Pinckney Jr, J. L. (1989). Tidally induced estuarine phytoplankton patchiness. *Limnology and Oceanography, 34*(2), 410-419.

Egert-Berg, K., Hurme, E. R., Greif, S., Goldstein, A., Harten, L., Flores-Martínez, J. J., . . . Borissov, I. (2018). Resource ephemerality drives social foraging in bats. *Current Biology, 28*(22), 3667-3673. e3665.

Fiedler, P. C., Reilly, S. B., Hewitt, R. P., Demer, D., Philbrick, V. A., Smith, S., . . . Mate, B. R. (1998). Blue whale habitat and prey in the California Channel Islands. *Deep-Sea Research Part II, 45*(8-9), 1781-1801.

Findlay, K. P., Seakamela, S. M., Meÿer, M. A., Kirkman, S. P., Barendse, J., Cade, D. E., . . . Wilke, C. G. (2017). Humpback whale "super-groups" – A novel low-latitude feeding behaviour of Southern Hemisphere humpback whales (*Megaptera novaeangliae*) in the Benguela Upwelling System. *PLoS ONE, 12*(3), e0172002. doi: doi:10.1371/journal.pone.0172002

Flanagan, T. P., Letendre, K., Burnside, W., Fricke, G. M., & Moses, M. (2011). *How ants turn information into food.* Paper presented at the 2011 IEEE symposium on artificial life (ALIFE).

Fossette, S., Abrahms, B., Hazen, E. L., Bograd, S. J., Zilliacus, K. M., Calambokidis, J., . . . Croll, D. A. (2017). Resource partitioning facilitates coexistence in sympatric cetaceans in the California Current. *Ecology and evolution, 7*(21), 9085-9097.

Fournet, M. E., Matthews, L. P., Gabriele, C. M., Mellinger, D. K., & Klinck, H. (2018). Source levels of foraging humpback whale calls. *The Journal of the Acoustical Society of America, 143*(2), EL105-EL111.

Fournet, M. E., Szabo, A., & Mellinger, D. K. (2015). Repertoire and classification of non-song calls in Southeast Alaskan humpback whales (*Megaptera novaeangliae*). *The Journal of the Acoustical Society of America, 137*(1), 1-10.

Friedlaender, A. S., Bowers, M. T., Cade, D., Hazen, E. L., Stimpert, A. K., Allen, A. N., . . . Goldbogen, J. A. (2020). The advantages of diving deep: Fin whales quadruple their energy intake when targeting deep krill patches. *Functional Ecology, 34*(2), 497-506.

Gero, S., & Whitehead, H. (2016). Critical decline of the Eastern Caribbean sperm whale population. *PloS one, 11*(10), e0162019.

Giraldeau, L.-A., & Caraco, T. (2000). Ch 8- Social Patch and Prey Models *Social Foraging Theory* (pp. 205-226). Princeton, NJ, USA: Princeton University Press.

Goldbogen, J. A., Cade, D. E., Wisniewska, D. M., Potvin, J., Segre, P. S., Savoca, M. S., . . . Pyenson, N. D. (2019). Why whales are big but not bigger: Physiological drivers and ecological limits in the age of ocean giants. *Science, 366*, 1367-1372.

Goldbogen, J. A., Friedlaender, A. S., Calambokidis, J., McKenna, M. F., Simon, M., & Nowacek, D. P. (2013). Integrative approaches to the study of baleen whale diving behavior, feeding performance, and foraging ecology. *BioScience, 63*(2), 90-100.

Gordon, D. M. (2014). The ecology of collective behavior. *PLoS Biol, 12*(3), e1001805.

Gordon, D. M., Rosengren, R., & Sundström, L. (1992). The allocation of foragers in red wood ants. *Ecological entomology, 17*(2), 114-120.

Gridley, T., Silva, M., Wilkinson, C., Seakamela, S., & Elwen, S. (2018). Song recorded near a super-group of humpback whales on a mid-latitude feeding ground off South Africa. *The Journal of the Acoustical Society of America, 143*(4), EL298-EL304.

Haury, L., McGowan, J., & Wiebe, P. (1978). Patterns and processes in the time-space scales of plankton distributions *Spatial pattern in plankton communities* (pp. 277-327): Springer.

Hazen, E. L., Friedlaender, A. S., & Goldbogen, J. A. (2015). Blue whale (*Balaenoptera musculus*) optimize foraging efficiency by balancing oxygen use and energy gain as a function of prey density. *Science Advances, 1*, e1500469. doi: 10.1126/sciadv.1500469

Hazen, E. L., Friedlaender, A. S., Thompson, M. A., Ware, C. R., Weinrich, M. T., Halpin, P. N., & Wiley, D. N. (2009). Fine-scale prey aggregations and foraging ecology of humpback whales *Megaptera novaeangliae*. *Mar Ecol Prog Ser, 395*, 75-89.

Hein, A. M., & Martin, B. T. (2020). Information limitation and the dynamics of coupled ecological systems. *Nature Ecology & Evolution, 4*(1), 82-90. doi: 2397-334X

Hofmann, E. E., & Murphy, E. J. (2004). Advection, krill, and Antarctic marine ecosystems. *Antarctic Science, 16*(4), 487-499.

Huang, H. C., Joseph, J., Huang, M. J., & Margolina, T. (2016). *Automated detection and identification of blue and fin whale foraging calls by combining pattern recognition and machine learning techniques.* Paper presented at the OCEANS 2016 MTS/IEEE Monterey.

Hucke-Gaete, R., Osman, L. P., Moreno, C. A., Findlay, K. P., & Ljungblad, D. K. (2004). Discovery of a blue whale feeding and nursing ground in southern Chile. *Proceedings of the Royal Society of London. Series B: Biological Sciences, 271*(suppl_4), S170-S173.

Irvine, L. M., Palacios, D. M., Lagerquist, B. A., & Mate, B. R. (2019). Scales of blue and fin whale feeding behavior off California, USA, with implications for prey patchiness. *Frontiers in Ecology and Evolution, 7*, 338.

Jarvis, T., Kelly, N., Kawaguchi, S., van Wijk, E., & Nicol, S. (2010). Acoustic characterisation of the broad-scale distribution and abundance of Antarctic krill (*Euphausia superba*) off East Antarctica (30-80 E) in January-March 2006. *Deep Sea Research Part II: Topical Studies in Oceanography, 57*(9), 916-933.

Johannes, R., Squire, L., Graham, T., Sadovy, Y., & Renguul, H. (1999). Spawning aggregations of groupers (Serranidae) in Palau. *The nature conservancy marine research series publication, 1*, 1-144.

Johnson, D. D., Kays, R., Blackwell, P. G., & Macdonald, D. W. (2002). Does the resource dispersion hypothesis explain group living? *Trends in Ecology & Evolution, 17*(12), 563-570.

Johnston, D., Thorne, L., & Read, A. (2005). Fin whales *Balaenoptera physalus* and minke whales *Balaenoptera acutorostrata* exploit a tidally driven island wake ecosystem in the Bay of Fundy. *Marine Ecology Progress Series, 305*, 287-295.

Jurasz, C. M., & Jurasz, V. P. (1979). Feeding modes of the humpback whale (*Megaptera Novaeangliae*) in southeast Alaska. *Scientific Reporting of Whales Research Institute, 31*, 69-83.

Kahane-Rapport, S. R., & Goldbogen, J. A. (2018). Allometric scaling of morphology and engulfment capacity in rorqual whales. *Journal of Morphology*, 1-13.

Kahane-Rapport, S. R., Savoca, M. S., Cade, D. E., Segre, P. S., Bierlich, K. C., Calambokidis, J., . . . Goldbogen, J. A. (2020). Lunge filter feeding biomechanics constrain rorqual foraging ecology across scale. *Journal of Experimental Biology, jeb.224196* doi: 10.1242/jeb.224196

Kawamura, A. (1980). A review of food of balaenopterid whales. *Scientific Reports of the Whales Research Institute, 32*, 155-197.

Kirchner, T., Wiley, D. N., Hazen, E. L., Parks, S. E., Torres, L. G., & Friedlaender, A. S. (2018). Hierarchical foraging movement of humpback whales relative to the structure of their prey. *Marine Ecology Progress Series, 607*, 237-250.

Lang, S. D., & Farine, D. R. (2017). A multidimensional framework for studying social predation strategies. *Nature ecology & evolution, 1*(9), 1230-1239.

LaScala-Gruenewald, D. E., Mehta, R. S., Liu, Y., & Denny, M. W. (2019). Sensory perception plays a larger role in foraging efficiency than heavy-tailed movement strategies. *Ecological Modelling, 404*, 69-82.

Laskowski, K. L., & Bell, A. M. (2014). Strong personalities, not social niches, drive individual differences in social behaviours in sticklebacks. *Animal Behaviour, 90*, 287-295.

Laundré, J. W. (2010). Behavioral response races, predator–prey shell games, ecology of fear, and patch use of pumas and their ungulate prey. *Ecology, 91*(10), 2995-3007.

Lévy, M., Franks, P. J., & Smith, K. S. (2018). The role of submesoscale currents in structuring marine ecosystems. *Nature communications, 9*(1), 1-16.

Littaye, A., Gannier, A., Laran, S., & Wilson, J. P. (2004). The relationship between summer aggregation of fin whales and satellite-derived environmental conditions in the northwestern Mediterranean Sea. *Remote Sensing of Environment, 90*(1), 44-52.

Livoreil, B., & Giraldeau, L.-A. (1997). Patch departure decisions by spice finches foraging singly or in groups. *Animal behaviour, 54*(4), 967-977.

Lomac-MacNair, K., & Smultea, M. A. (2016). Blue whale (Balaenoptera musculus) behavior and group dynamics as observed from an aircraft off Southern California. *Animal Behavior and Cognition, 3*(1), 1-21.

Magurran, A. E. (1990). The adaptive significance of schooling as an anti-predator defence in fish. *Annales Zoologici Fennici, 27*, 51-66.

Mastick, N. (2016). *The Effect of Group Size on Individual Roles and the Potential for Cooperation in Group Bubble-net Feeding Humpback Whales (Megaptera novaeangliae).* M.S., Oregon State University, Corvallis, OR.

Mate, B. R., Lagerquist, B. A., & Calambokidis, J. (1999). Movements of north pacific blue whales during the feeding season off southern california and their southern fall migration1. *Marine Mammal Science, 15*(4), 1246-1257.

McNamara, J. M., & Houston, A. I. (1990). State-dependent ideal free distributions. *Evolutionary Ecology, 4*(4), 298-311.

Miller, E., Potts, J., Cox, M., Miller, B., Calderan, S., Leaper, R., . . . Double, M. (2019). The characteristics of krill swarms in relation to aggregating Antarctic blue whales. *Scientific Reports, 9*(1), 1-13.

Newton, K. M., & DeVogelaere, A. (2013). Marine mammal and seabird abundance and distribution around the Davidson Seamount, July 2010. *Monterey Bay National Marine Sanctuary Technical Report*.

Nicol, S., James, A., & Pitcher, G. (1987). A first record of daytime surface swarming by *Euphausia lucens* in the Southern Benguela region. *Marine Biology, 94*(1), 7-10.

Nowacek, D. P., Friedlaender, A. S., Halpin, P. N., Hazen, E. L., Johnston, D. W., Read, A. J., . . . Zhu, Y. (2011). Super-aggregations of krill and humpback whales in Wilhelmina Bay, Antarctic Peninsula. *PLoS One, 6*(4), e19173.

Oestreich, W. K., Fahlbusch, J. A., Cade, D. E., Calambokidis, J., Margolina, T., Joseph, J., . . . Ryan, J. P. (2020). Animal-borne metrics enable acoustic detection of blue whale migration. *Current Biology, 30*, 1-7.

Oleson, E. M., Calambokidis, J., Burgess, W. C., McDonald, M. A., LeDuc, C. A., & Hildebrand, J. A. (2007). Behavioral context of call production by eastern North Pacific blue whales. *Marine Ecology-Progress Series, 330*.

Oleson, E. M., Wiggins, S. M., & Hildebrand, J. A. (2007). Temporal separation of blue whale call types on a southern California feeding ground. *Animal Behaviour, 74*(4), 881-894.

Oliver, M. J., Kohut, J. T., Bernard, K., Fraser, W., Winsor, P., Statscewich, H., . . . Carvalho, F. (2019). Central place foragers select ocean surface convergent features despite differing foraging strategies. *Scientific reports, 9*(1), 157.

Owen, K., Kavanagh, A. S., Warren, J. D., Noad, M. J., Donnelly, D., Goldizen, A. W., & Dunlop, R. A. (2017). Potential energy gain by whales outside of the Antarctic: prey preferences and consumption rates of migrating humpback whales (*Megaptera novaeangliae*). *Polar Biology, 40*(2), 277-289.

Paduan, J. D., & Rosenfeld, L. K. (1996). Remotely sensed surface currents in Monterey Bay from shore-based HF radar (Coastal Ocean Dynamics Application Radar). *Journal of Geophysical Research: Oceans, 101*(C9), 20669-20686.

Page, R. A., & Bernal, X. E. (2020). The challenge of detecting prey: Private and social information use in predatory bats. *Functional Ecology, 34*(2), 344-363.

Parker, G. A., & Stuart, R. A. (1976). Animal behavior as a strategy optimizer: evolution of resource assessment strategies and optimal emigration thresholds. *The American Naturalist, 110*(976), 1055-1076.

Parrish, J. K., & Edelstein-Keshet, L. (1999). Complexity, pattern, and evolutionary trade-offs in animal aggregation. *Science, 284*(5411), 99-101.

Peikert, R., Pobitzer, A., Sadlo, F., & Schindler, B. (2014). A comparison of finite-time and finite-size Lyapunov exponents *Topological Methods in Data Analysis and Visualization III* (pp. 187-200): Springer.

Piatt, J. F., & Methven, D. A. (1992). Threshold foraging behavior of baleen whales. *Marine Ecology Progress Series, 84*, 205-210.

Pineda, J., Starczak, V., da Silva, J. C., Helfrich, K., Thompson, M., & Wiley, D. (2015). Whales and waves: Humpback whale foraging response and the shoaling of internal waves at S tellwagen B ank. *Journal of Geophysical Research: Oceans, 120*(4), 2555-2570.

Pirotta, V., Owen, K., Donnelly, D., Brasier, M. J., & Harcourt, R. (2021). First evidence of bubble-net feeding and the formation of 'super-groups' by the east Australian population of humpback whales during their southward migration. *Aquatic Conservation: Marine and Freshwater Ecosystems*.

Potvin, J., Cade, D. E., Werth, A. J., Shadwick, R. E., & Goldbogen, J. A. (2020). A perfectly inelastic collision: bulk prey engulfment by baleen whales and dynamical implications for the world's largest cetaceans. *American Journal of Physics, 88*(10), 851-863.

Pöysä, H. (1992). Group foraging in patchy environments: the importance of coarse-level local enhancement. *Ornis scandinavica*, 159-166.

Ramm, C. (2018). *Animal congregation in the open ocean-a theoretical approach.* Christian-Albrechts Universität Kiel.

Roeleke, M., Blohm, T., Hoffmeister, U., Marggraf, L., Schlägel, U. E., Teige, T., & Voigt, C. C. (2020). Landscape structure influences the use of social information in an insectivorous bat. *Oikos*.

Ross-Marsh, E., Elwen, S., Prinsloo, A., James, B., & Gridley, T. (2020). Singing in South Africa: monitoring the occurrence of humpback whale (*Megaptera novaeangliae*) song near the Western Cape. *Bioacoustics*, 1-17.

Ryan, J. P., Cline, D. E., Dawe, C., McGill, P., Zhang, Y., Joseph, J., . . . DeVogelaere, A. (2016). *New Passive Acoustic Monitoring in Monterey Bay National Marine Sanctuary.* Paper presented at the OCEANS 2016 MTS/IEEE Monterey, CA, USA.

Ryan, J. P., Cline, D. E., Joseph, J. E., Margolina, T., Santora, J. A., Kudela, R. M., . . . Michisaki, R. (2019). Humpback whale song occurrence reflects ecosystem variability in feeding and migratory habitat of the northeast Pacific. *PloS one, 14*(9).

Santora, J. A., Field, J. C., Schroeder, I. D., Sakuma, K. M., Wells, B. K., & Sydeman, W. J. (2012). Spatial ecology of krill, micronekton and top predators in the central California Current: Implications for defining ecologically important areas. *Progress in Oceanography, 106*, 154-174.

Santora, J. A., Zeno, R., Dorman, J. G., & Sydeman, W. J. (2018). Submarine canyons represent an essential habitat network for krill hotspots in a large marine ecosystem. *Scientific reports, 8*(1), 7579.

Scales, K. L., Miller, P. I., Hawkes, L. A., Ingram, S. N., Sims, D. W., & Votier, S. C. (2014). On the Front Line: frontal zones as priority at-sea conservation areas for mobile marine vertebrates. *Journal of Applied Ecology, 51*(6), 1575-1583.

Scales, K. L., Schorr, G. S., Hazen, E. L., Bograd, S. J., Miller, P. I., Andrews, R. D., . . . Falcone, E. A. (2017). Should I stay or should I go? Modelling year-round habitat suitability and drivers of residency for fin whales in the California current. *Diversity and Distributions, 23*(10), 1204-1215.

Schmidt, K. A., Dall, S. R., & Van Gils, J. A. (2010). The ecology of information: an overview on the ecological significance of making informed decisions. *Oikos, 119*(2), 304-316.

Schoenherr, J. R. (1991). Blue whales feeding on high concentrations of euphausiids around Monterey Submarine Canyon. *Canadian Journal of Zoology, 69*(3), 583-594.

Shadden, S. C., Lekien, F., & Marsden, J. E. (2005). Definition and properties of Lagrangian coherent structures from finite-time Lyapunov exponents in two-dimensional aperiodic flows. *Physica D: Nonlinear Phenomena, 212*(3-4), 271-304.

Shadden, S. C., Lekien, F., Paduan, J. D., Chavez, F. P., & Marsden, J. E. (2009). The correlation between surface drifters and coherent structures based on high-frequency radar data in Monterey Bay. *Deep Sea Research Part II: Topical Studies in Oceanography, 56*(3-5), 161-172.

Slater, G. J., Goldbogen, J. A., & Pyenson, N. D. (2017). Independent evolution of baleen whale gigantism linked to Plio-Pleistocene ocean dynamics. *Proc. R. Soc. B, 284*(1855), 20170546.

Stafford, K. M., Fox, C. G., & Clark, D. S. (1998). Long-range acoustic detection and localization of blue whale calls in the northeast Pacific Ocean. *The Journal of the Acoustical Society of America, 104*(6), 3616-3625.

Swartz, S. L., & Jones, M. L. (1981). Demographic studies and habitat assessment of gray whales, Eschrichtius robustus. *Laguna San Ignacio, Baja California Sur, Mexico*.

Torney, C. J., Berdahl, A., & Couzin, I. D. (2011). Signalling and the evolution of cooperative foraging in dynamic environments. *PLoS computational biology, 7*(9).

Valeix, M., Chamaillé-Jammes, S., & Fritz, H. (2007). Interference competition and temporal niche shifts: elephants and herbivore communities at waterholes. *Oecologia, 153*(3), 739-748.

van der Hoop, J., Nousek-McGregor, A., Nowacek, D., Parks, S., Tyack, P., & Madsen, P. (2019). Foraging rates of ram-filtering North Atlantic right whales. *Functional Ecology, 33*(7), 1290-1306.

Visser, F., Hartman, K. L., Pierce, G. J., Valavanis, V. D., & Huisman, J. (2011). Timing of migratory baleen whales at the Azores in relation to the North Atlantic spring bloom. *Marine Ecology Progress Series, 440*, 267-279.

Warren, J. D., & Demer, D. A. (2010). Abundance and distribution of Antarctic krill (Euphausia superba) nearshore of Cape Shirreff, Livingston Island, Antarctica, during six austral summers between 2000 and 2007. *Canadian Journal of Fisheries and Aquatic Sciences, 67*(7), 1159-1170.

Weinrich, M. T., Schilling, M. R., & Belt, C. R. (1992). Evidence for acquisition of a novel feeding behaviour: lobtail feeding in humpback whales, Megaptera novaeangliae. *Animal behaviour, 44*(6), 1059-1072.

Wessel, P., & Smith, W. H. (1996). A global, self-consistent, hierarchical, high-resolution shoreline database. *Journal of Geophysical Research: Solid Earth, 101*(B4), 8741-8743.

Whitehead, H. (1983). Structure and stability of humpback whale groups off Newfoundland. *Canadian Journal of Zoology, 61*(6), 1391-1397.

Wiley, D. N., Ware, C., Bocconcelli, A., Cholewiak, D., Friedlaender, A., Thompson, M., & Weinrich, M. (2011). Underwater components of humpback whale bubble-net feeding behavior. *Behaviour, 148*, 575-602.

Wilson, R. P., Neate, A., Holton, M. D., Shepard, E. L., Scantlebury, D. M., Lambertucci, S. A., . . . Marks, N. (2018). Luck in food finding affects individual performance and population trajectories. *Current Biology, 28*(23), 3871-3877. e3875.

Witek, Z., Kalinowski, J., & Grelowski, A. (1988). Formation of Antarctic krill concentrations in relation to hydrodynamic processes and social behaviour *Antarctic Ocean and resources variability* (pp. 237-244): Springer.